



TECHNICAL UNIVERSITY OF LIBEREC
Faculty of Mechatronics, Informatics
and Interdisciplinary Studies ■

Effect of selected types of nanoparticles on natural bacterial communities in soil and in wastewater treatment plants

Master thesis

Study programme: N3942 – Nanotechnology

Study branch: 3942T002 – Nanomaterials

Author: **Bc. Filip Hrnčířík**

Supervisor: RNDr. Alena Ševců, Ph.D.







TECHNICKÁ UNIVERZITA V LIBERCI
Fakulta mechatroniky, informatiky
a mezipřoborových studií ■

Vliv vybraných typů nanočástic na přirozené bakteriální komunity v půdě a v čistírnách odpadních vod

Diplomová práce

Studijní program: N3942 – Nanotechnologie

Studijní obor: 3942T002 – Nanomateriály

Autor práce: **Bc. Filip Hrnčířk**

Vedoucí práce: RNDr. Alena Ševců, Ph.D.





ZADÁNÍ DIPLOMOVÉ PRÁCE

(PROJEKTU, UMĚLECKÉHO DÍLA, UMĚLECKÉHO VÝKONU)

Jméno a příjmení: **Bc. Filip Hrnčířík**
Osobní číslo: **M15000007**
Studijní program: **N3942 Nanotechnologie**
Studijní obor: **Nanomateriály**
Název tématu: **Vliv vybraných typů nanočástic na přirozené bakteriální komunity v půdě a v čistírnách odpadních vod.**
Zadávací katedra: **Ústav nových technologií a aplikované informatiky**

Z á s a d y p r o v y p r a c o v á n í :

1. Vypracovat literární rešerši k zadané problematice. Zdrojem informací budou především vědecké články dostupné na běžných vyhledávačích: Web of Science, Scopus, Google Scholar.
2. Naučit se techniku FISH (fluorescence in situ hybridisation) pro detekci různých skupin půdních bakterií.
3. Provést laboratorní testy s vybranými typy půd a nZVI v různém uspořádání v mikrokosmech.
4. Analyzovat výsledky pomocí fluorescenčního mikroskopu a analýzy obrazu.
5. Studovat vliv nanočástic Ag a TiO₂ na bakteriích aktivovaného kalu, bakteriálním biofilmu a na vybraných bakteriálních kulturách (Paracoccus, Nitrosomonas, Thauera).
6. Naučit se analýzu vzorku (oxidy dusíku, plynný dusík a kyslík) pomocí plynového chromatografu a chemiluminiscenčního analyzátoru (NO).
7. Výsledky upravit do grafické podoby, okomentovat a srovnat je s dostupnou literaturou.

Rozsah grafických prací: dle potřeby
Rozsah pracovní zprávy: 70 - 90 stran
Forma zpracování diplomové práce: tištěná/elektronická
Jazyk zpracování diplomové práce: Angličtina

Seznam odborné literatury:

- [1] ČERNÍK, Miroslav. Chemicky podporované in situ sanační technologie. Praha: Vydavatelství VŠCHT, 2010. ISBN 978-80-7080-767-5.
- [2] BRIDGER, Joanna M. a Emanuela V. VOLPI. Fluorescence in situ hybridization (FISH): protocols and applications. New York, NY: Humana Press, c2010. Springer protocols, v. 659. ISBN 978-1-60761-789-1.
- [3] FAJARDO, C., L.T. ORTÍZ, M.L. RODRÍGUEZ-MEMBIBRE, M. NANDE, M.C. LOBO a M. MARTIN. Assessing the impact of zero-valent iron (ZVI) nanotechnology on soil microbial structure and functionality: A molecular approach. Chemosphere [online]. 2012, 86(8), 802-808 [cit. 2017-10-13]. DOI: 10.1016/j.chemosphere.2011.11.041. ISSN 00456535. Dostupné z: <http://linkinghub.elsevier.com/retrieve/pii/S0045653511013336>
- [4] SCHLICH, Karsten, Thorsten KLAWONN, Konstantin TERYTZE a Kerstin HUND-RINKE. Hazard assessment of a silver nanoparticle in soil applied via sewage sludge. Environmental Sciences Europe [online]. 2013, 25(1), 17- [cit. 2017-10-13]. DOI: 10.1186/2190-4715-25-17. ISSN 2190-4715. Dostupné z: <http://enveurope.springeropen.com/articles/10.1186/2190-4715-25-17>
- [5] ANON., 2016. Nanomaterials in Waste Streams [online]. B.m.: OECD Publishing [vid. 2017-10-13]. ISBN 978-92-64-24061-2. Dostupné z: http://www.oecd-ilibrary.org/environment/nanomaterials-in-waste-streams_9789264249752-en

Vedoucí diplomové práce: RNDr. Alena Ševců, Ph.D.
Ústav nových technologií a aplikované informatiky


Konzultant diplomové práce: Dr. Claire Courtis
NIBIO

Ostatní konzultanti: Carmen Fajardo, Ph.D.
Universidad Complutense Madrid

Datum zadání diplomové práce: 19. října 2017
Termín odevzdání diplomové práce: 14. května 2018


prof. Ing. Zdeněk Plíva, Ph.D.
děkan

L.S.


Ing. Josef Novák, Ph.D.
vedoucí ústavu

V Liberci dne 19. října 2017



Declaration

I hereby certify that I have been informed that Act 121/2000, the Copyright Act of the Czech Republic, namely Section 60, School-work, applies to my master thesis in full scope. I acknowledge that the Technical University of Liberec (TUL) does not infringe my copyrights by using my master thesis for TUL's internal purposes.

I am aware of my obligation to inform TUL on having used or licensed to use my master thesis in which event TUL may require compensation of costs incurred in creating the work at up to their actual amount.

I have written my master thesis myself using literature listed therein and consulting it with my supervisor and my tutor.

I hereby also declare that the hard copy of my master thesis is identical with its electronic form as saved at the IS STAG portal.

Date: 14.5.2018

Signature: 

Acknowledgements

I would like to express thanks to all people who participated directly or indirectly in this work. Special thanks go to dr. Alena Sevcu for her patience, advices and given opportunities to work abroad, dr. Carmen Fajardo and whole Madrid group for their help with FISH analysis, dr. Lucie Svobodova for her limitless patience and help with the image analysis, dr. Claire Courtis for her advices and guidance in gas chromatography and nitric oxide analysis, Lukas Varaja for his help and proofreading. Finally, I would like to thank my family, Interstellar 7 and Karen Restrepo Avila for their support throughout the creation of this study.



Abstract

This master thesis is focused on the investigation of effect of titanium dioxide, silver and zero-valent iron nanoparticles on distinct bacterial strains and communities from the wastewater treatment plants and soil. A gas chromatography and a nitric oxide analysis were conducted in order to study possible impact of titanium dioxide and silver nanoparticles on the process of denitrification and nitrification of single bacterial strains (*Thauera linaloolentis*, *Paracoccus denitrificans* and *Nitrosomonas europaea*) and bacterial communities present in the activated sludge and biofilms of municipal wastewater treatment plants. The effect of nanoscale zero-valent iron on the bacterial consortium present in the soil was addressed using fluorescence *in situ* hybridisation method in a 28-days experiment. Following bacterial groups were analysed: *Proteobacteria* (α , β , γ), *Firmicutes*, *Actinobacteria* and the domain of *Eubacteria*. Titanium dioxide nanoparticles did not reveal any significant impact on the respiration process of denitrifying bacteria. Silver nanoparticles had negative effect on the oxygen respiration and nitrite production by nitrifying bacteria at the highest tested concentrations (0.1 and 1 mg/L). Combination of titanium dioxide and silver nanoparticles showed no substantial effect on the respiration kinetics of the bacterial biofilm or the activated sludge. Fluorescence *in situ* hybridisation unveiled shifts in the structure of soil microbial communities after the exposure to selected nano zero-valent iron nanoparticles.

Key words:

titanium dioxide, silver, nZVI, nanoparticles, *Thauera linaloolentis*, *Paracoccus denitrificans*, *Nitrosomonas europaea*, activated sludge, biofilm, FISH



Abstrakt

Tato diplomová práce je zaměřená na vliv nanočástic oxidu titaničitého, stříbra a nulmocného železa na vybrané bakteriální kmeny a bakteriální společenstva vyskytující se v čistírnách odpadních vod a v půdě. Pro studium vlivu nanočástic oxidu titaničitého a stříbra na proces denitrifikace a nitrifikace jednotlivých bakteriálních kmenů (*Thauera linaloolentis*, *Paracoccus denitrificans* a *Nitrosomonas europaea*) a bakteriálních společenstev, které se vyskytují v aktivovaném kalu a biofilmu čistíren odpadních vod, byla použita plynová chromatografie a analýza oxidu dusnatého. Vliv nanočástic nulmocného železa na půdní bakteriální společenstva byl sledován pomocí metody fluorescenční *in situ* hybridizace po dobu 28 dní. Zkoumány byly následující bakteriální skupiny: *Proteobacteria* (α , β , γ), *Firmicutes*, *Actinobacteria* a doména *Eubacteria*. Nanočástice oxidu titaničitého neměly žádný významný vliv na respirační procesy denitrifikačních bakterií. Nanočástice stříbra negativně ovlivnily proces respirace kyslíku a produkce dusitanu u nitrifikačních bakterií pouze při nejvyšších testovaných koncentracích (0.1 a 1 mg/L). Žádný významný vliv nanočástic oxidu titaničitého a stříbra na respiraci bakteriálního biofilmu a aktivovaného kalu nebyl detekován. Fluorescenční *in situ* hybridizace ukázala změny ve struktuře půdních bakteriálních společenstev po vystavení vybraným druhům nanočástic nulmocného železa.

Klíčová slova:

oxid titaničitý, stříbro, nZVI, nanočástice, *Thauera linaloolentis*, *Paracoccus denitrificans*, *Nitrosomonas europaea*, aktivovaný kal, biofilm, FISH



Contents

1	Introduction	21
2	Materials and methods	27
2.1	Nanoparticles	27
2.2	Effect of <i>TiO₂</i> and <i>Ag</i> nanoparticles on bacteria from activated sludge and biofilms	31
2.2.1	Bacterial cultures and communities	31
2.2.2	Experimental design	32
2.2.3	Analytical methods	37
2.3	Effect of nZVI nanoparticles on bacterial soil communities	39
2.3.1	Experimental design	39
2.3.2	Fluorescence <i>in situ</i> hybridisation	41
2.3.3	Image analysis	42
2.4	Statistical analysis	46
3	Results and discussion	47
3.1	Effect of <i>TiO₂</i> and <i>Ag</i> NPs on bacteria from WWTPs	47
3.1.1	Effect of <i>TiO₂</i> NPs on denitrifying bacteria	47
3.1.2	Effect of <i>Ag</i> NPs on nitrifying bacteria	50



3.1.3	Effect of TiO_2 and <i>Ag</i> NPs on bacterial community in biofilm	52
3.1.4	Effect of TiO_2 and <i>Ag</i> NPs on bacterial community in activated sludge	56
3.2	Effect of nZVI on soil bacteria	59
3.2.1	Image analysis of FISH data	59
3.2.2	Comparison of BC-nZVI and NANOFER 25S impact	61
4	Conclusions	65
	Bibliography	67
	Appendix	78



List of Figures

2.1	Representative TEM image of dispersed TiO_2 NPs (left); scale bar is 500 nm. Detail of TiO_2 aggregates (right). Both images were provided by the JRC.	28
2.2	Representative TEM images of Ag nanospheres. Both images were provided by Nanocomposix.	29
2.3	SEM image of nZVI on carbon particle; scale bar is 1 μm . Image was provided by RCPTM.	30
2.4	SEM image of NANOFER 25S aggregated particles; scale bar is 500 nm. The slurry was dried before the SEM imaging, therefore it may not accurately reflect the size of the original material [44].	30
2.5	Adjustment of image from fluorescence microscope: (A) original image; (B) image after adjustment and calibration of background. . . .	45
2.6	Image with identified objects - red, green and yellow objects were included; blue circled objects were excluded from the analysis.	45
3.1	Time course of respiration of O_2 by <i>P. denitrificans</i> after exposure to various concentrations of TiO_2 NPs. Error bars represent SD of triplicate samples.	48
3.2	Time course of respiration of O_2 by <i>T. linaloolentis</i> after exposure to various concentrations of TiO_2 NPs. Error bars represent SD of triplicate samples.	49



3.3	Time course of respiration of O_2 by <i>N. europaea</i> after exposure to various concentrations of <i>Ag</i> NPs. Error bars represent SD of duplicate samples.	50
3.4	Time course of production of N_2 by bacterial consortium from biofilm after exposure to TiO_2 NPs. Error bars show SD of duplicate samples.	53
3.5	Time course of production of N_2 by bacterial consortium from biofilm after exposure to <i>Ag</i> NPs.	54
3.6	Time course of production of N_2 by bacterial consortium from biofilm after exposure to combination of TiO_2 and <i>Ag</i> NPs. Error bars are SD of duplicate samples.	54
3.7	Time course of production of N_2 by bacteria community located in activated sludge after exposure to TiO_2 NPs and combination of TiO_2 and <i>Ag</i> NPs.	57
3.8	The phylogenetic microbial composition as detected by FISH.	62
B1	Evacuation and a helium-filling semi-automated system for GC analysis.	82
B2	Stainless steel gas-tight reactors for biofilm testing.	83
B3	Improved version of robotised gas analysis system [39].	83
B4	Demonstration of the intermediate phase that consisted of 400 μL of the cell layer.	84
B5	The falcon tube with the filtration paper ready for the filter entry. . .	84
B6	Filters prepared for hybridisation.	85
B7	Fluorescence microscope (AxioImager, ZEISS, Germany).	85



C1	Kinetics of the respiration of <i>P. denitrificans</i> after exposure to TiO_2 NPs. Each plot represents one sample.	88
C2	Kinetics of the respiration of <i>T. linaloolentis</i> after exposure to TiO_2 NPs with concentration of 0.01 and 0.1 mg/L . Each plot represents one sample.	89
C3	Kinetics of the respiration of <i>T. linaloolentis</i> after exposure to TiO_2 NPs with concentration of 1 and 10 mg/L . Each plot represents one sample.	90
C4	Kinetics of the respiration of <i>N. europaea</i> after exposure to <i>Ag</i> NPs with concentration of 0.1 and 1 $\mu g/L$. Each plot represents one sample.	91
C5	Kinetics of the respiration of <i>N. europaea</i> after exposure to <i>Ag</i> NPs with concentration of 10 and 1000 $\mu g/L$. Each plot represents one sample.	92
C6	Kinetics of the respiration of bacterial consortium located in biofilm after exposure to TiO_2 NPs with various concentrations. Each plot represents one sample.	93
C7	Kinetics of the respiration of bacterial consortium located in biofilm after exposure to <i>Ag</i> NPs with various concentrations. Each plot represents one sample.	94
C8	Kinetics of the respiration of bacterial consortium located in biofilm after exposure to combination of TiO_2 and <i>Ag</i> NPs with various concentrations. Each plot represents one sample.	95
C9	Kinetics of the respiration of bacterial community located in activated sludge after exposure to TiO_2 and combination of TiO_2 and <i>Ag</i> NPs with various concentrations. Each plot represents one sample.	96



List of Tables

A1	Sistrom's medium	78
A2	Trace elements and vitamins solution for <i>Paracoccus's</i> medium	79
A3	Thauera's medium	79
A4	Basal salts medium	80
A5	Modified trace elements solution for <i>Nitrosomonas's</i> medium	80
A6	The main characteristics of the soil.	81
A7	Synthetic wastewater solution	81
D1	Analysis of 95% O_2 consumption by <i>P. denitrificans</i> after exposure to TiO_2 NPs in time. No significant variation was observed.	97
D2	Analysis of 95% O_2 consumption by <i>T. linaloolentis</i> after exposure to TiO_2 NPs in time. No significant variation was detected.	97
D3	Analysis of NO maximal accumulation by <i>P. denitrificans</i> after exposure to TiO_2 NPs in time. No significant variation was observed.	98
D4	Analysis of NO maximal accumulation by <i>T. linaloolentis</i> after exposure to TiO_2 NPs in time. No significant variation was observed.	98
D5	Analysis of 90% O_2 consumption by <i>N. europaea</i> after exposure to Ag NPs in time. No significant variation was detected between 0.1 - 10 $\mu g/L$ concentrations. NC = no consumption.	98



D6	Analysis of NO_2^- maximal accumulation by <i>N. europaea</i> after exposure to <i>Ag</i> NPs in time. No significant variation was observed between 0.1 - 10 $\mu g/L$. LV = significantly low values.	98
D7	Analysis of times when more than 95% of N_2 was accumulated by bacterial consortium from biofilm after exposure to TiO_2 NPs. No significant variation was detected.	99
D8	Analysis of NO maximal accumulation by bacterial consortium from biofilm after exposure to TiO_2 NPs in time. No significant variation was observed.	99
D9	Analysis of NO_2^- maximal accumulation by bacterial consortium from biofilm after exposure to TiO_2 NPs in time. No significant variation was observed.	99
D10	Analysis of times when more than 95% of N_2 was accumulated by bacterial consortium from biofilm after exposure to <i>Ag</i> NPs. No significant variation was detected.	99
D11	Analysis of NO maximal accumulation by bacterial consortium from biofilm after exposure to <i>Ag</i> NPs in time. No significant variation was observed. X = sample problem.	100
D12	Analysis of NO_2^- maximal accumulation by bacterial consortium from biofilm after exposure to <i>Ag</i> NPs in time. No significant variation was noticed.	100
D13	Analysis of times when more than 95% of N_2 was accumulated by bacterial consortium from biofilm after exposure to combination of TiO_2 and <i>Ag</i> NPs. No significant variation was detected.	100



D14 Analysis of NO maximal accumulation by bacterial consortium from biofilm after exposure to combination of TiO_2 and Ag NPs in time. No significant variation was observed. 101

D15 Analysis of NO_2^- maximal accumulation by bacterial consortium from biofilm after exposure to combination of TiO_2 and Ag NPs in time. No significant variation was noticed. 101

D16 Analysis of times when more than 95% of N_2 was accumulated by bacteria community located in activated sludge after exposure to TiO_2 and combination of TiO_2 and Ag NPs without control sample. Weird control not included in the statistical analysis (red). 101



List of abbreviations

Ag NPs	silver nanoparticles
NO	nitric oxide
TiO ₂ NPs	titanium dioxide nanoparticles
BC-nZVI	biochar nanoscale zero-valent iron
BrdU	5-bromo-2-deoxy-uridine
COD	chemical oxygen demand
DAPI	4'-6-diamidino-2-phenylindole
DI water	deionised water
FISH	fluorescence <i>in situ</i> hybridisation
GC	gas chromatography
ICP-OES	inductively coupled plasma atomic emission spectroscopy
LDH	lactate dehydrogenase
LECA	Light Expanded Clay Aggregate
MTT	3-(4,5-dimethylthiazol-2-yl)-2,5-diphenyltetrazolium bromide
NADH, NAD ⁺	oxidised and reduced form of nicotinamide adenine dinucleotide
NMs	nanomaterials
NPs	nanoparticles
nZVI	nanoscale zero-valent iron
OD	optical density



PBS	phosphate-buffered saline
RCPTM	Regional Centre of Advanced Technologies and Materials
ROS	reactive oxygen species
SBR	sequencing batch reactor
SD	standard deviation
SDS	sodium dodecyl sulfate
SWW	synthetic wastewater
WWTPs	wastewater treatment plants
XTT	2,3-bis (2-methoxy-4-nitro-5-sulfophenyl)-5-[(phenylamino) carbonyl]- 2H-tetrazolium hydroxide



1 Introduction

Nowadays, nanomaterials (NMs) are commonly used in many different industries around the world. Whether they are silver nanoparticles (*Ag* NPs) for their antimicrobial properties [1, 2], nanoparticles of titanium dioxide (*TiO₂* NPs) for photocatalytic applications [3, 4], nanoscale zero-valent iron (nZVI) for decontamination [5, 6] or others, this besides all the positive properties means that NMs are also part of the industrial pollution.

The introduction of NMs to the environment could be done in several ways. First of all, it is crucial to differentiate between conscious and unconscious intrusion.

In the first case, we usually talk about nZVI and its abilities in fields of decontamination and remediation of soil [7] and groundwater [6, 8]. Among other methods, adsorption technique using the nZVI has been considered simple and effective tool for the removal of heavy metal ions from wastewater due to its wide adaptability, environment-friendly usage and low cost [9, 10, 11].

On the other hand, extensive use of NMs such as *TiO₂* nanostructures due to their alluring material properties and applications in numerous fields as optical devices and sensors [12], photocatalysis [4, 13], antibacterial coatings, organic pollutants [14, 15] and others NMs in consumer products such as appliances, textiles, electronics and computers, home furnishing, motor vehicles and health [16], has resulted in their tremendous leakage into environment and finding their way to landfills, incineration plants and wastewater treatment plants (WWTPs). Therefore, microorganisms, which are responsible for the removal of organic nitrogen in WWTPs, are constantly exposed to a broad range of “new” contaminants. In order to provide satisfactory water quality standards, it is necessary to ensure that these contaminants, such as NMs, do not compromise the biological processes carried out in the WWTPs.

Another problem could arise, if NMs elude all the processes and stay in the sewage sludge – usually in a new form, for example, *Ag* NPs in form of sulphides (*Ag₂S*)



[17, 18]. As sludge is commonly applied to an agricultural land as a fertiliser [19], plants might take up and store those NPs and their transformation products from the soil. This could be a potential way for NMs to get into the human food chain and cause additional harm [18, 19].

Although several studies proved that the toxicity of NMs is decreasing over time in sewage sludge [20, 21], the impacts on the removal of organic nitrogen from wastewater and the possible toxic effects of NMs on the bacteria themselves, remain unclear.

Moreover, application of nZVI in the decontamination of organic pollutants in aquatic and soil environments is rising. In order to apply nZVI safely, it is essential to investigate its possible harm on bacterial cultures living in these environments.

Several analytical assessments could be provided in order to investigate influence of NMs in different environments. *In vitro* tests are widely used. Their advantages lay in requiring only small amount of testing material; limitation of toxic waste; speed, price and reproducibility of experiment; and mainly in maintaining control of conditions and environment throughout the whole process of examination [22].

Assessment techniques are often divided into groups by aspects of approach. For instance, cell viability is the group where ratio of live/dead cells, growth rate, proliferation, apoptosis and necrosis are closely explored [23]. Subsequently, it is crucial to understand toxicity mechanisms by examination of oxidative stress and DNA damage of the testing subjects.

MTT and XTT are widespread proliferation assays where a cellular reduction of tetrazolium salts produces formazan dyes. These dyes are then detected by optical absorbance and utilised as an indicator of cell metabolism. This method requires minimal physical manipulation of model cells and generate quick and reproducible results. Nevertheless, the understanding of results could be misleading, for example, due to the reaction of tetrazolium salts with NPs [24].

Correspondingly, [³H]thymidine incorporation and Alamar Blue (known as *resazurin*



test) are based on metabolism of model organism. In the case of [^3H]thymidine, radioactively labelled thymidine is incorporated in freshly synthesised DNA. It is utterly accurate method for detection of cell proliferation but due to its high price and possible *in vitro* toxicity it is usually avoided [22]. Alamar blue is a non-fluorescent dye which is reduced in viable cells to soluble resorufin. In contrast, resorufin is extremely fluorescent. Still, NPs could react with it and therefore compromise the results [25].

In addition, supravital dyes, namely, Trypan Blue, Neutral Red and propidium iodide assess membrane integrity as a tool to determine cellular viability. Both trypan blue and propidium iodide are molecules with charge which do not enter cell freely. However, damaged cells have disrupted membranes and thus the entrance is achievable [26]. After the access of dyes, each cell fluorescents with slightly different wavelength. Alternatively, Neutral Red is uncharged molecule which can access both live/dead cells but only inside the living cell fluorescents in specific wavelength. This is viable solely due to the change of pH which allows protonation of Neutral Red by acidic lysosomes [27].

Another approach could be taken by using LDH (lactate dehydrogenase) which is an oxido-reductive stable enzyme presented in almost all organisms. It catalyses the interconversion of pyruvate and lactate with concomitant interconversion of NADH and NAD^+ . Now, if a tissue or a cell is spoiled by toxic material, it releases LDH into its surrounding. With regard to its stability, it is conceivable to identify it in higher levels. As for colorimetric LDH tests, reduction of MTT in NADH-coupled enzymatic reaction to form of reduced MTT is used [28].

Naturally, it is vital to observe any potential interference between NPs and assay components which could lead to decrease in the test accuracy. Unfortunately, recognition of such interference is difficult to predict and might often occur [29].

In order to investigate cell death as a result of action of NPs, it is desirable to apply assays which include inspection of single cells changes, for instance, TUNEL assay

[30] and annexin-V assay [31].

The TUNEL assay manipulates with double-strand breakage and DNA fragmentation during the process of apoptosis. DNA polymerase is consistently used along with BrdU (5-bromo-2-deoxy-uridine) which is fused with the repaired double-strand breaks inside the cells. Subsequently, anti-BrdU antibody is joined to the incorporated BrdU in respect of labelling the DNA. This implies that they are likely to be detected via the microscope.

Moreover, annexin-V is a phosphatidylserine specific binding substrate which operates the phosphatidylserine located on the surface of the cell during apoptotic restructuring of membrane. The substrate can be labelled by a fluorescence dye to draw attention to membrane in early and late state of apoptosis [23].

Genotoxicity and DNA damage are often inspected by the single cell gel electrophoresis assay (SCGE) also known as COMET assay [32]. Cells embedded in agarose gel are lysed with detergent and high salt to form a nucleoid. Afterwards, the nucleoid is tagged by ethidium bromide and separated by process of electrophoresis. A fluorescence microscope then indicates the damage of DNA by amount of DNA fragments [33].

Different approaches could be employed in order to examine effect of NMs on organisms living in soil or groundwater. Interest is focused on the abundance structure of microbial community and its function throughout the experimental period.

Specifically, total cell number expressed, e.g. as number of bacteria per *mL* or *L* in liquid samples or per *g* of dry weight in soil samples, can be determined by direct counting using DAPI (4'-6-diamidino-2-phenylindole) staining as a DNA fluorescence agent. Cell viability, besides other methods, is assessed using a two-dye fluorescent bacterial viability kit that distinguish viable (commonly green) and dead (red) cells under a fluorescence microscope. Afterwards, it is possible to calculate live and dead cells abundance.

Another technique for evaluation of toxicity of NPs in soil applies the Luria-Bertani agar plates. In this simple assessment, the treated bacteria are after the incubation



period compared to the control bacteria (without treatment) by counting the number of colony forming units on the plates [34]. The problem is that the cultivability of bacteria from soil samples ranges between 0.1 and 1.5% [35]. Therefore, composition of the soil microbial communities are often analysed in the soil by FISH (fluorescence *in situ* hybridisation).

One of the key features of this technique is the ability to observe each individual cell and therefore know what exactly is happening in certain time. Application of proper probes and protocols [36, 37] is vital in this case. Although this method is more time consuming due to the microscopy and image analysis process, it can give detailed information about the real structure of the targeted microbial groups [38] and might bring more precise information than molecular biology techniques that rely on proper DNA extraction. FISH method was used in this study, therefore further explanation will be provided in chapter Material and methods.

Furthermore, inductively coupled plasma atomic emission spectroscopy (ICP-OES) is relevant analytical technique for detection of chemical elements. This method allows to analyse almost all elements of the periodic table, that could be transformed in solution, with sensitivity to units of *ppb* to hundreds of units of *ppm* [17, 18, 19]. The ability to evaluate gas production/reduction during the period of an experiment that investigates an effect of NPs is a significant advantage. Therefore, gas chromatography (GC) is broadly used and its mechanised modifications are utterly popular [19, 39, 40]. For instance, by monitoring nitric oxide (*NO*) it is achievable to study denitrification as well as other bacterial *NO* transformations. *NO* is known as a vital signal molecule [41], an agent in interactions amid pathogenic bacteria and microbiota [42], and, for example, a releasing agent of other molecules [43].

This thesis is focused on the effect of several types of NPs on different bacterial strains and communities living in environments such as WWTPs and soil.

Firstly, a potential toxic effect of *TiO₂* and *Ag* NPs on bacteria was studied. Particularly, single strain denitrifiers *Thauera linaloolentis* and *Paracoccus denitrificans*, single strain nitrifiers *Nitrosomonas europaea*, and more complex bacterial commu-

nities present in the activated sludge and biofilms of municipal WWTPs were examined. Both complexes were examined to elucidate NPs impact on the process of denitrification.

Secondly, an investigation of toxic effect of nZVI on bacterial community present in the soil was addressed using the FISH method in a 28-days experiment. Following bacterial groups were analysed: *Proteobacteria* (α , β , γ), *Firmicutes*, *Actinobacteria* and the domain of *Eubacteria*.



2 Materials and methods

2.1 Nanoparticles

Two different types of NPs were used in the WWTPs assessments: titanium dioxide NPs (TiO_2 NPs, JRC ID: JRCNM01001a, obtained from the Joint Research Centre (JRC), Ispra, Italy) and silver NPs (Ag NPs, obtained from Nanocomposix, San Diego, USA).

Titanium dioxide NPs were uncoated anatase particles with a primary particle size of 5-8 nm measured by the JRC using the small-angle X-ray scattering (SAXS) and TEM (see Figure 2.1). Based on the information provided by the JRC, the number of dispersed aggregates and agglomerates smaller than 100 nm was 95.2%, smaller than 50 nm was 77.3% and smaller than 10 nm was 10.7% (measured by TEM). The surface area was $316.1 \text{ m}^2/\text{g}$ (measured by BET).



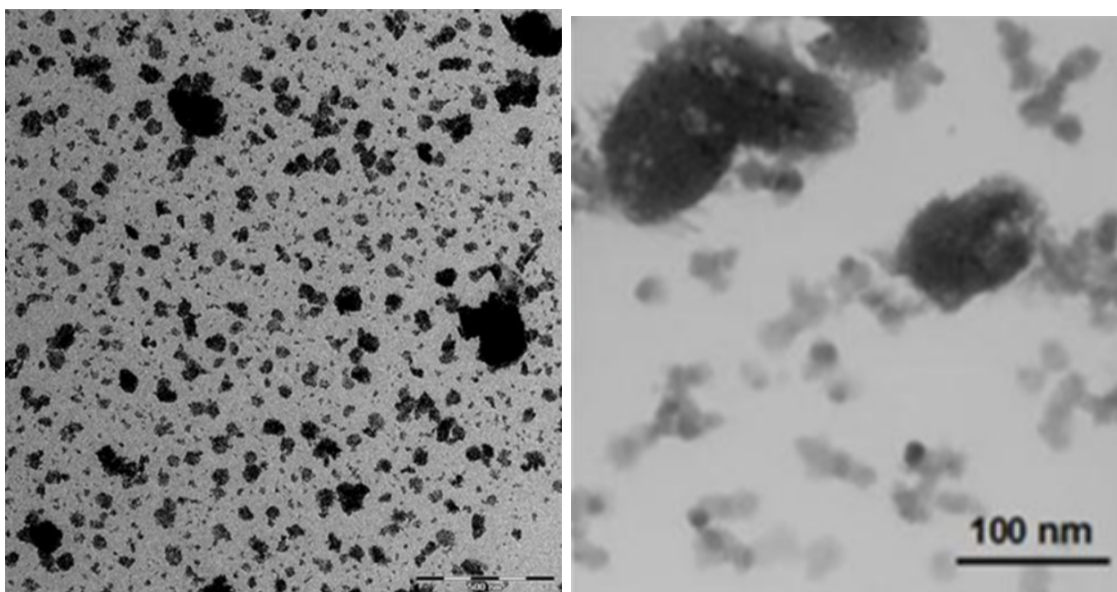


Figure 2.1: Representative TEM image of dispersed TiO_2 NPs (left); scale bar is 500 nm. Detail of TiO_2 aggregates (right). Both images were provided by the JRC.

The NPs were received in a powder form and subsequently suspended in a deionised (DI) water by sonication following the NANoREG protocol for producing reproducible dispersions of engineered NMs in exposure media. Suspended NPs were then stored at 4°C in darkness.

Ag NPs had a primary particle size around 21.2 ± 7.9 nm (see Figure 2.2), a surface area of 21.3 m^2/g and hydrodynamic diameter in water equal to 41.5 nm. These NPs were coated with polyvinylpyrrolidone (PVP).

The NPs were received as a stable suspension with a nominal concentration of 5.2 g/L. The NPs were kept at 4°C in darkness before testing.



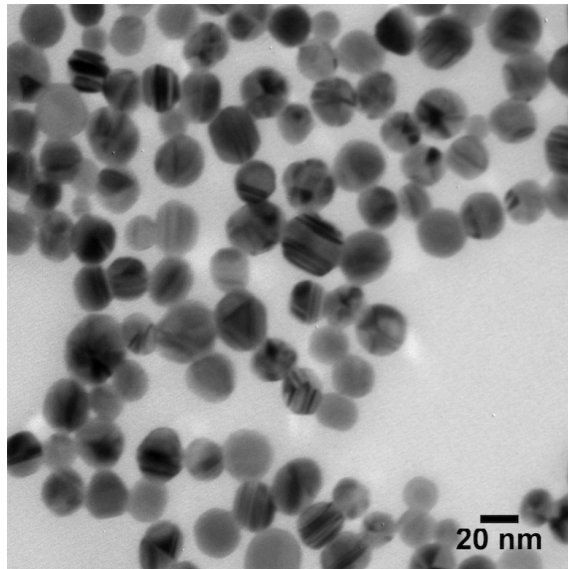


Figure 2.2: Representative TEM images of *Ag* nanospheres. Both images were provided by Nanocomposix.

In FISH assessments were examined following NPs: BC-nZVI (batch 14-H, obtained from Regional centre of advanced technologies and materials, RCPTM), Palacky University Olomouc, Czech Republic) and NANO FER 25S (obtained from NANO IRON s.r.o., Czech Republic).

BC-nZVI consisted of three phases: α -Fe (35%), γ -Fe (13%) and C-graphite (51%). Its quantification and parameters were set by Rietveld analysis. The surface area was approximately $184 \text{ m}^2/\text{g}$ (see Figure 2.3).

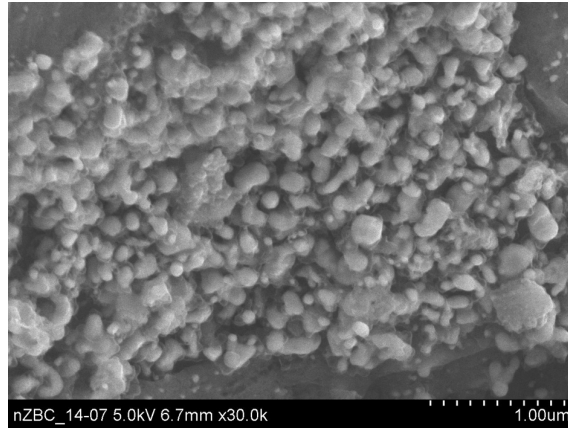


Figure 2.3: SEM image of nZVI on carbon particle; scale bar is 1 μm . Image was provided by RCPTM.

NANOFER 25S was used as an aqueous dispersion of stabilised nZVI (coated with sodium polyacrylic acid 3%) with average particle size $<50\text{ nm}$ and specific surface $>25\text{ m}^2/\text{g}$ (Figure 2.4). NANOFER 25S was composed of iron (14-18%), magnetite (Fe_3O_4 ; 6-2%), carbon (0-1%), water (77%) and surfactant (3%).

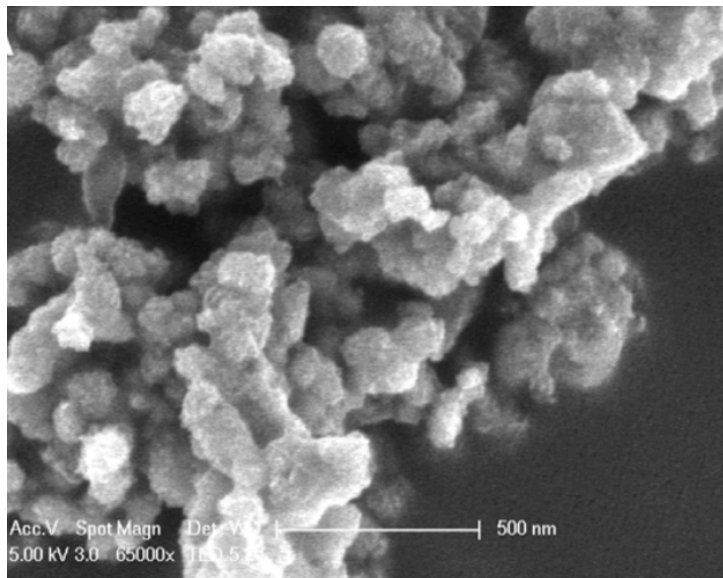


Figure 2.4: SEM image of NANOFER 25S aggregated particles; scale bar is 500 nm . The slurry was dried before the SEM imaging, therefore it may not accurately reflect the size of the original material [44].



2.2 Effect of TiO_2 and Ag nanoparticles on bacteria from activated sludge and biofilms

The examination of single strain denitrifiers, nitrifiers and complex bacterial communities obtained from activated sludge and biofilms of municipal WWTPs with TiO_2 and Ag NPs is described in this section.

2.2.1 Bacterial cultures and communities

Single bacterial strains were obtained from the German Collection of Microorganisms and Cell Cultures (Leibniz Institute DSMZ, Braunschweig, Germany), namely, *Paracoccus denitrificans* (DSM-413), *Thauera linaloolentis* (DSM-12138) and *Nitrosomonas europaea* (DSM-28437).

Paracoccus denitrificans is a gram-negative, non-motile, denitrifying bacterium with a typically rod-shaped cells. It belongs to the class of α -*Proteobacteria*. This bacterium is a model organism for studying denitrification and can be commonly found in WWTPs, where it reduces nitrate to nitrogen gas. Metabolically, it can grow as a chemolithoautotroph (carbon dioxide used as an inorganic energy source)[45]. Strain was isolated from activated sludge and its optimal growth temperature is around 20°C.

P. denitrificans was cultivated in Sistrom's medium ([46]; see Table A1) with an initial pH of 7.3. In addition, trace elements solution and vitamins solution (see Table A2) were added. pH was adjusted to 7.3 with 10 M *KOH* and the medium was sterilised in autoclave.

Thauera linaloolentis is a gram-negative, mesophilic, motile bacterium. It belongs to the class of β -*Proteobacteria*. This bacterium is exhibiting a rapid complete onset (RCO) denitrifying phenotype, which means that it can shift rapidly from oxic to

anoxic respiration [47]. The optimal growth temperature is around 25°C.

T. linaloolentis was cultivated in Thauera's medium ([47]; see Table A3) with an initial pH of 7.6. The medium was subsequently autoclaved for sterility.

Nitrosomonas europaea is a gram-negative obligate chemolithoautotroph which derives all energy for growth from the oxidation of ammonia to nitrite. It belongs to the class of β -*Proteobacteria*. *N. europaea* participates in the biogeochemical nitrogen cycle in the process of nitrification – the conversion of reduced nitrogen in the form of ammonia [NH_3] or ammonium [NH_4^-] to oxidised nitrogen in the form of nitrate [NO_3^-], nitrite [NO_2^-], or gaseous forms [NO , N_2O]. The optimal growth temperature is around 15°C.

N. europaea was cultivated in basal salts medium (see Table A4 with an initial pH of 7.8. In addition, solution of modified trace elements (see Table A5) was added. pH was adjusted to 7.8 and the medium was sterilised in autoclave. Additionally, the medium was filter-sterilised before inoculation by the bacterium.

Natural bacterial communities were obtained from actively operating WWTPs (BEVAS and VEAS in Oslo, Norway). In the case of BEVAS, I operated with their activated sludge which was freshly sampled on the day of the experiment. More information about BEVAS WWTPs can be found at: <http://www.bvas.no>

In the case of VEAS, biofilm associated bacteria present on the LECA (Light Expanded Clay Aggregate) particles was sampled from the denitrification tank and stored (4°C) few days before the realisation of the experiment. Additional information about VEAS WWTPs can be found at: <http://www.veas.no>

2.2.2 Experimental design

Seven separate experiments were performed: six of them dealt with an impact of NPs on the process of denitrification and one experiment dealt with the process of nitrification. Each of them is described in detail below.



Effect of TiO₂ NPs on denitrifying bacteria

Firstly, the toxic impact of *TiO₂* NPs on the single bacterium strain *P. denitrificans* was examined. Assays were performed in 120 mL vials under a vigorous stirring (750 rpm, triangular stirring bar 25 x 8 mm). Each vial contained 40 mL of the Sistrom's medium, 0.9 mL of bacterial culture (OD₆₆₀ - 0.1), a specific volume of *TiO₂* NPs to reach exact concentration and additional DI water to fulfil the final sample volume of 50 mL. Investigated concentrations were in a range of 0.1 mg/L up to 10 mg/L with a factor of 10 between them. Dilution of *TiO₂* NPs was made in DI water. In addition, 100 µL of 1 M *KNO₃* was added to each vial to set the final concentration of *NO₃⁻* to 2 mM. The vials were crimped with a butyl septa and aluminium caps. Prior to the inoculation, the air was replaced with helium during six cycles of a evacuation and a helium-filling using a semi-automated system ([39]; see Figure B1). During this process, the medium in the vials was stirred at 950 rpm to ensure sufficient gas exchange between liquid and gas phases. Thereafter, the excess pressure of each vial was released using a ethanol-filled syringe where the piston was removed. In addition, 1 mL of *O₂* was added in each vial to adjust the final concentration of *O₂* to 1 % w/v. Immediately after, 0.9 mL of bacterial culture was added to all of the vials. The GC bath was set to 20°C and the frequency of gas sampling was set to every 2 hours. After the vials reached the equal temperature, the excess pressure was released again. Thereafter, the gas analysis started.

Secondly, the toxic impact of *TiO₂* NPs on a single strain bacterium *T. linaloolentis* was investigated. This experiment was set in the same conditions as the one with *P. denitrificans*. Tested concentrations were in a range of 10 µg/L up to 10 mg/L with a factor of 10 between them, the GC bath was set to 25°C and the frequency of gas sampling was set to every 2.4 hours.

All samples were measured in triplicates. Sterile environment was maintained throughout the whole process.



Effect of Ag NPs on N. europaea

Assays were performed in 120 mL vials under stirring (200 rpm, triangular stirring bar 25 x 8 mm). Each vial was sterilised by 1 M HCl and subsequently autoclaved. The basal salts medium was filter-sterilised before adding into fresh autoclaved vials. Each vial contained 1 mL of the bacterial culture, a specific volume of Ag NPs to reach exact concentration and the basal salts medium to fulfil the final sample volume of 50 mL. Investigated concentrations were in a range of 0.1 µg/L up to 1 mg/L with a factor of 10 between them. The dilution of Ag NPs was made in the basal salts medium. In addition, 25 µL of Phenol red (pH indicator, pink at neutral pH and turning yellow at lower pH) was added to each vial to stain the growing bacterial culture. A special septa with teflon on one side together with aluminium caps were sterilised by an ethanol and an UV light (15 minutes) before crimping the vials. Prior to the inoculation, the air was replaced with helium during six cycles of the evacuation and the helium-filling using a semi-automated system. During this process, the medium in the vials was stirred at 950 rpm to ensure sufficient gas exchange between liquid and gas phases. Thereafter, the excess pressure of each vial was released using an ethanol-filled syringe where the piston was removed. In addition, 3.5 mL of O₂ was added in each vial to adjust the final concentration of O₂ to 5% v/v. Immediately after, 1 mL of the bacterial culture was added to all of the vials. The GC bath was set to 30°C and the frequency of gas sampling was set to every 6 hours. After the vials reached the equal temperature, the excess pressure was released again and 0.6 mL of the liquid sample for NO₂⁻ analysis were taken from each vial. After 120 hours, 1 mL of 0.1 M NH₄Cl was added to each vial to set the final concentration of NH₄⁺ to 2 mM. In addition after 168 hours, 0.1 mL of 0.1 M NaHCO₃ and 1 mL of 0.1 M NH₄Cl were added to each vial in order to feed the bacterial culture. All samples were examined in duplicates. Sterile environment was maintained throughout the whole process.



Effect of TiO_2 and Ag NPs on bacterial biofilm

The effect of Ag NPs on a complex of bacterial communities that formed a biofilm on the surface of the porous LECA particles (VEAS, Oslo, Norway) was examined. LECA particles were stored in dark cold (4°C) place and activated by mixing with synthetic wastewater (SWW, see Table A7) for 30 minutes before the experiment started. Assays were performed in 145 mL stainless steel gas-tight reactors with stirring (950 rpm, triangular stirring bar 25 x 8 mm, see Figure B2). Each reactor was composed of 6 g of LECA particles, a specific volume of Ag NPs to reach exact concentration and SWW to fulfil the final sample volume of 65 mL. Investigated concentrations were 0.1 and 1 mg/L of Ag NPs. The dilution of Ag NPs was made in SWW. LECA particles were situated on the nonmagnetic metal screen (1 mm-diameter pores) approximately one centimeter above the bottom of reactor to ensure proper flow of liquid [48]. The reactor openings were crimped with a butyl septa and aluminium caps. The air was replaced with helium during six cycles of the evacuation and the helium-filling using a semi-automated system. The GC bath was set to 15°C and the frequency of gas sampling was set to every 1.2 hours. After the reactors reached the equal temperature, the excess pressure was released and 0.6 mL of the liquid sample for NO_2^- analysis were taken. Thereafter, 0.65 mL of 0.1 mM KNO_3 was added to each reactor to adjust the final concentration of NO_3^- to 1 mM. 30 minutes later, the second liquid samples were taken. Since then, liquid samples for NO_2^- analysis were taken every hour until the quantity of NO_2^- plummeted.

Furthermore, the impact of TiO_2 NPs was investigated following the same protocol as for Ag. The only difference was that the investigated concentrations were 1 and 10 mg/L of TiO_2 NPs.

In addition, the impact of the combination of TiO_2 NPs and Ag NPs was tested. The conditions of the assessment were the same as the ones above with only difference being that the investigated concentrations were combinations of 0.1 mg/L of Ag NPs and 1 mg/L of TiO_2 NPs and subsequently 1 mg/L of Ag NPs and



10 mg/L of TiO_2 .

All samples were prepared in duplicates. Since I worked with LECA particles, which are commonly used in the WWTPs, it was not necessary to work in a sterile environment.

Effect of TiO_2 and Ag NPs on bacterial community in activated sludge

The effect of TiO_2 NPs and subsequently the combination of TiO_2 NPs and Ag NPs on a complex of bacterial communities presented in the activated sludge (BEVAS, Oslo, Norway) was examined. Activated sludge was freshly sampled and stored inside the cold box (4°C) for a few hours before the experiment started. Assays were performed in 120 mL vials with stirring (750 rpm, triangular stirring bar 25 x 8 mm). Each vial was composed of 40 mL of an activated sludge (pH 7), 8 mL of SWW (pH 7.7, source of carbon, see Table A7), a specific volume of TiO_2 and Ag NPs to reach exact concentration and DI water to fulfil the final sample volume of 50 mL. SWW was freshly prepared before the experiment. Investigated concentrations were 0.1 mg/L and 1 mg/L for TiO_2 NPs and as well for the combination of TiO_2 NPs and Ag NPs. Dilutions of TiO_2 NPs and Ag NPs were made in DI water. The vials were crimp-sealed with a butyl septa and aluminium caps. The air was replaced with helium during six cycles of the evacuation and the helium-filling using the semi-automated system. The GC bath was set to 16°C and the frequency of gas sampling was set to every 2.4 hours. After the vials reached the equal temperature, the excess pressure was released. In addition, 100 µL of 1 M KNO_3 was added to each of vials to set the final concentration of NO_3^- to 2 mM. No O_2 was added. All samples were tested in triplicates. Since I worked with the activated sludge, it was not necessary to work in a sterile environment.



2.2.3 Analytical methods

An improved version of robotised gas analysis system by Molstad et al. (2007) was used for gas analysis (see Figure B3) [39]. The application of gas chromatography (GC) was primarily designed for characterising of microbial communities (such as denitrifying bacteria) based on their gas production/reduction (O_2 , NO , N_2O and N_2), hence electron flows to the different electron acceptors, during and after the transition from oxic to anoxic conditions. The incubation system was composed of a thermostated water bath with positions for 30 crimp-sealed serum flasks (120 mL) and a magnetic stirring (Variomag HP 15, art no 41500 from H+P Labortechnik GmbH, Munich Germany) controlled by a Variomag Telemodul 40 S (H+P Labortechnik GmbH, Munich, Germany) [39]. The headspace gas was sampled periodically by an Agilent CTC GC-PAL autosampler and a Gilson Minipuls 3 peristaltic pump. The outlet from the sampling loop of the GC carried the gas with a He-flow (24 mL/min) to the open inlet of a chemiluminescence NO analyser (Sievers NOA 280i, Teledyne instrument, Norway). The GC (Agilent 7890A) was equipped with various valves, columns (molesieve column for separation of N_2 and O_2 , PLOTQ column for separation of CH_4 , N_2O and CO_2) and detectors such as Thermal Conductivity Detector (TCD) for a detection of a higher concentration of N_2O , Flame Ionisation Detector (FID) for a sensitive detection of CH_4 and Electron Captured Detector (ECD) for more sensitive measurement of N_2O (proportionally lower concentration than TCD), to analyse all relevant gases by a single injection.

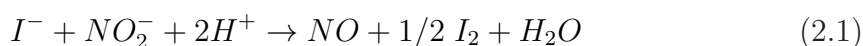
In short: Samples were taken from the headspace of 120 mL serum vials using an autosampler connected to a peristaltic pump. The autosampler operated a needle which pierced the septa on the vials (never twice at the same spot), and the pump took approximately one 1 mL of headspace gas from the vials into the sample loops of the GC and the NO analyser. After the injection the pump was reversed, pumping helium and the portion of the up-pumped gas in the pipelines back into the vials,



thus minimising dilution of the gas in the vials while maintaining atmospheric pressure [49].

The NO_2^- measurement was performed by using the sodium iodide (1 % w/v in 50 % acetic acid) that worked as a reducing agent of NO [50]. Subsequently, NO was analysed using the chemiluminescence NO analyser (Sievers NOA 280i, Teledyne instrument, Norway). This suitable and accurate method measures the NO_2^- down to nanomolar levels.

A liquid sample (0.6 mL) was centrifuged at 13400 rpm (12000*g) for 2 minutes using the MiniSpin centrifuge (Eppendorf). An aliquot of supernatant (200 μ L) was then stored in Eppendorf tubes at 4°C in the dark before further analysis. The supernatant was stirred for approximately 30 seconds right before the NO_2^- analysis. Thereafter, 10 μ L of supernatant was injected into the system via the injection port with the septa where the reducing agent immediately reduced the injected NO_2^- to the NO gas following this reaction:



The produced NO gas was subsequently transferred via a tubing into the chemiluminescence NO analyser where it was measured.

Raw data from GC was firstly refined by Calculus excel sheet (authors: prof. Lars Bakken, dr. Daniel Mania, Norwegian University of Life Sciences). Therefore, the results of the analysis of gas kinetics data took into account both the solubility of the gas and diffusion properties and were corrected for the dilution and the leakage.

Figures with error bars are displayed as mean of triplicate or duplicate samples with standard deviation (SD). Each detailed gas figure was statistically analysed in every inspected time and compared to control sample. In addition, statistical analysis of times when depletion (less than 95%) or accumulation (more than 95%) of investigated gases occurred was conducted.



2.3 Effect of nZVI nanoparticles on bacterial soil communities

In this section, the experiment with bacterial soil communities and NPs, namely, BC-nZVI and NANOFER 25S, is described. FISH method was applied for the evaluation of possible effect on the bacterial community.

2.3.1 Experimental design

The experiment was established in this order - two selected materials, BC-nZVI and NANOFER 25S, were mixed with 50 g of soil to reach 5% of the total weight. Control sample was prepared as a soil without any NPs. Sub-samples were taken in the beginning, after 8, 16 and 28 days.

Soil microcosms

Standard soil (batch 2.3, LUFA Speyer, Germany) was used, according to GLP (Good Laboratory Practice), in order to investigate influence of NPs on soil bacteria. This soil originated from naturally treated agricultural areas in Germany. The main physical-chemical characteristics are described in Table A6. Additional information can be found at: <http://www.lufa-speyer.de/>

50 g of soil was weighed in a 100 mL plastic vial. Subsequently, 20% suspension of NANOFER 25S (1 g of commercial suspension and 4 mL of DI water) and 11.1% suspension of BC-nZVI (1 g of NPs and 8 mL of DI water; dissimilar ratio due to a different structural composition) were separately prepared by mixing NPs with DI water and stirred thoroughly (Vortex genie 2, Scientific Industries, USA). To secure the nano-dimension of the particles in the suspension, ultrasound bath was applied for 15 minutes. Afterwards, 2.5 g of suspension of NANOFER 25S or BC-nZVI was



added into vials to form 5% of the total weight of the sample.

After the incubation period, enumeration of bacterial cells was performed in 1-g soil samples, according to published protocols [34, 36, 37].

Preparation of filtrates

1 g of soil sample was weighed on the laboratory weights (KERN 440-33N, Germany) and mixed with 11 mL of filter-sterilised phosphate-buffered saline (PBS) using the minishaker (lab dancer, IKA). The suspension was incubated overnight (37°C, 160 rpm) in orbital shaking incubator (INFORS AG CH-4103, Bottmingen, Switzerland).

Next day, the suspension was centrifuged for 10 minutes at 5000 rpm and 4°C (Universal 320R classic, Hettich lab technology, Germany) and the supernatant was discarded. Following that, the supernatant was replaced by 9 mL of filter-sterilised PBS containing 0.5% Tween 20, 2% formaldehyde and 10% SDS with a final pH of 7.4. The suspension was stirred vigorously and incubated in orbital shaking incubator overnight again.

Following day, the solution was mixed briefly for 15 minutes (Vortex genie 2, Scientific industries, USA). In order to detach and separate cells from inorganic particles, bacteria were extracted from soil slurries by density gradient centrifugation using the non-ionic medium OptiPrepTM Density Gradient Medium (Merck KGaA, Darmstadt, Germany, 60% (w/v) solution of iodixanol in sterile water, for further information visit: <https://www.sigmaaldrich.com>). Supernatant (3 mL) was transferred and gently stirred with 3 mL of OptiPrep using a syringe in a plastic tube. Then the centrifugation was applied for 99 minutes at 12000 rpm and 4°C. Approximately 400 µL of the cell layer (intermediate phase, see Figure B4), located just above the OptiPrep cushion, was thereafter taken and stored. To dilute and evenly distribute the cells on a filter paper, 900 µL of sterilised DI water was mixed with 100 µL of intermediate phase. Afterwards, 1 mL of sterilised DI water was added on a pre-



filter Qualitative filter paper (DP 597 055, 55 mm diameter, ALBET Labscience, Hahnemühle, Germany) combined with 0.2 μm polycarbonate filter (45 mm diameter, Isopore GTTP, Millipore, Germany) followed by 1 mL of prepared solution. The filtration was undertaken in gentle vacuum and then the filtrates were air-dried and stored at -20°C until further processing.

2.3.2 Fluorescence *in situ* hybridisation

Before the performance of FISH, the filters were cut into 0.15 cm^2 sections that were settled on a glass with parafilm in order to avoid movement of sample during the process of hybridisation.

The solution of proper probes and hybridisation buffer was vigorously stirred using the centrifuge (Denver instruments, USA). The filters were kept in closable 50 mL falcon tubes (see Figure B5) together with filtration papers which were soaked in humidity buffer (0.9 M NaCl, 20 mM Tris-*HCl* and DI water, pH 7). Since the phylogenetic probes were used, the hybridisation temperature and incubation time were set to 46°C and 90 minutes ([36]; see Figure B6). Afterwards, the filters were transferred into a pre-warmed vials containing 100 μL of washing buffer (0.9 NaCl, 20 mM Tris-*HCl*, 10% SDS, pH 7) and incubated at 46°C for 11 minutes. The same washing step was performed twice.

The hybridisation was performed using a combination of the specific Cy3-labelled probe that was special for each bacterial group, and the general FAM-labelled EUB338 bacterial probe as follows:

for α -*Proteobacteria* 30 μL of hybridisation buffer (0.9 M NaCl, 20 mM Tris-*HCl*, pH 7, 10% SDS, and 20% formamide) together with 5 μL of ALF1B probe (100 pmol/ μL final concentration) and 5 μL of EUB338 (100 pmol/ μL final concentration) were added on filter;

for β -*Proteobacteria* 25 μL of hybridisation buffer (0.9 M NaCl, 20 mM Tris-*HCl*, pH 7, 10% SDS, and 35% formamide) together with 5 μL of BET42a probe



(100 pmol/ μ L final concentration), 5 μ L of GAM42A (without fluorescence dye, 100 pmol/ μ L final concentration) and 5 μ L of EUB338 were added on filter; for γ -*Proteobacteria* 25 μ L of hybridisation buffer (0.9 M NaCl, 20 mM Tris-HCl, pH 7, 10% SDS, and 35% formamide) together with 5 μ L of GAM42a probe (100 pmol/ μ L final concentration), 5 μ L of BET42a (without fluorescence dye, 100 pmol/ μ L final concentration) and 5 μ L of EUB338 were added on filter; for *Actinobacteria* 30 μ L of hybridisation buffer (0.9 M NaCl, 20 mM Tris-HCl, pH 7, 10% SDS, and 25% formamide) together with 5 μ L of HGC69A probe (100 pmol/ μ L final concentration) and 5 μ L of EUB338 were added on filter; for *Firmicutes* 30 μ L of hybridisation buffer (0.9 M NaCl, 20 mM Tris-HCl, pH 7, 10% SDS, and 35% formamide) together with 5 μ L of LGC353a probe (100 pmol/ μ L final concentration) and 5 μ L of EUB338 were added on filter; and for domain of *Eubacteria* 25 μ L of hybridisation buffer (0.9 M NaCl, 20 mM Tris-HCl, pH 7, 10% SDS, and 20% formamide) together with 5 μ L of EUB338II probe (100 pmol/ μ L final concentration), EUB338III probe (100 pmol/ μ L final concentration) and 5 μ L of EUB338 were added on filter.

After hybridisation, each filter section was mounted using drops of Citifluor AF1 (antifading solution, Citifluor, United Kingdom) on a glass slide and explored with fluorescence microscope (AxioImager, ZEISS, Germany; see Figure B7). Autofluorescence of the cells was investigated using negative controls.

2.3.3 Image analysis

The evaluation of the FISH images was performed by program Matlab (The Mathworks) with Image Processing Toolbox. Image analysis processing was several times discussed with dr. Lucie Svobodova who is also the author of final script (length 940 rows).

Basic correlation of image background such as adjustment of brightness and contrast, balance of histogram were optimised based on literature overview [51, 52, 53].



Each image was divided into three colour components (RGB), namely red, green and blue. The yellow objects were evaluated by intersection of red and green components, i.e. the yellow object had to be in red and green layer simultaneously.

Each separated layer (red, green or blue) was basically greyscale image which consisted of 256 levels of grey. This layer was subsequently transformed into black and white image using the Otsu method. This is a thresholding method that determines boundaries of object/background (in this case cell/background) and provides a conversion of the image into binary one which has solely two levels of grey, white (values are equal to one) and black (values are equal to zero) respectively. Thresholding is a process where all pixels with a value of greyscale lower than a certain value (threshold) are changed to zero and all above this threshold are changed to 1. Black and white image is obtained and is composed of only two disjoint sets.

Objects that were excluded from the image analysis: 1) smaller or bigger than acceptable limit (the smaller ones corresponded to the limit of microscope detection, it was image noise; and the bigger ones were undesirable for the experiment); 2) objects that had a lower or higher brightness than a fixed limits (the lower limit was double of the brightness of background and the higher limit was arranged empirically by myself based on advices of an experience co-worker); 3) objects that had a low circularity (these were apparently not cells).

Number of objects was evaluated in each binary image (in each R-G-B layer and yellow objects separately) using the *"bwboundaries"* function. This function seeks for internal contours. In order to investigate area parameters such as area, diffusivity, circularity and directionality of the objects, the function *"regionprops"* was applied. The default units of parameters were pixels or after recalculation μm eventually. Results were summarised in excel file. An example of image analysis is illustrated in Figures 2.5 and 2.6.

Soil microbial population was inspected in the fluorescence microscope. 10 images were taken per each specific probe. Afterwards, the total number of *Eu-bacteria* (green objects) and the total number of specific bacterial group (yellow

objects - intersection of green and red objects) were evaluated by image analysis. The %-representation of specific bacterial group within the total number of *Eubacteria* was then calculated.



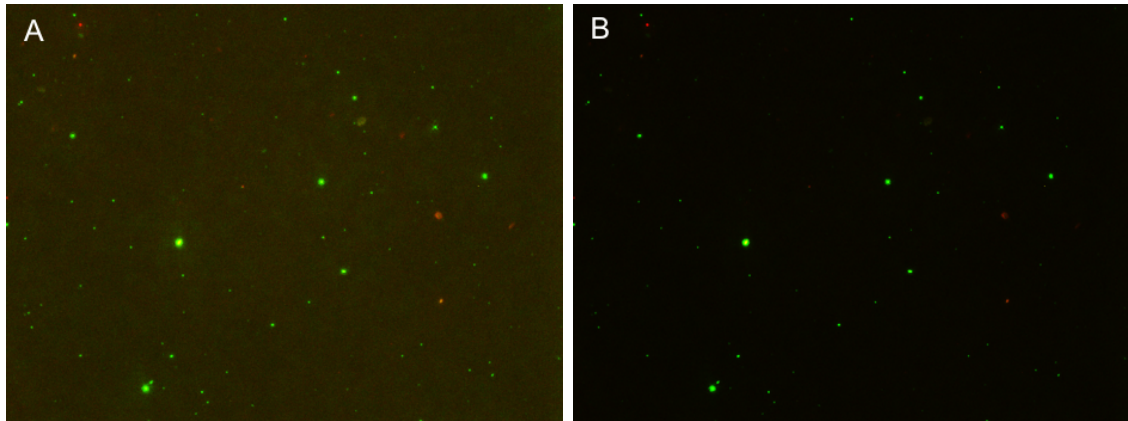


Figure 2.5: Adjustment of image from fluorescence microscope: (A) original image; (B) image after adjustment and calibration of background.

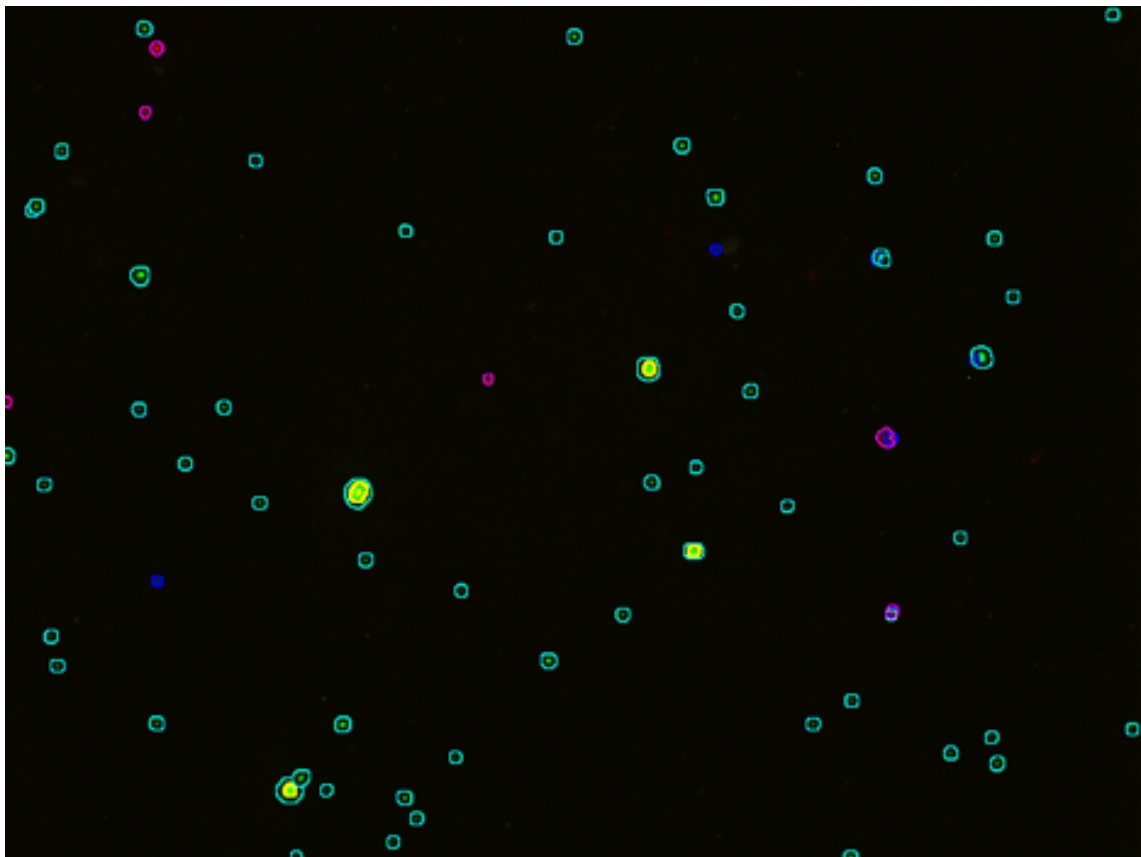


Figure 2.6: Image with identified objects - red, green and yellow objects were included; blue circled objects were excluded from the analysis.

2.4 Statistical analysis

Investigation of TiO_2 and Ag NPs impact on bacteria from WWTPs was statistically analysed by GraphPad PRISM 6. One-way or two-way (also called one-factor or two-factor) ANOVA test was applied depending on the data set. Furthermore, Dunnett's multiple comparisons test was used in order to compare each NPs concentration to control in specific time. Smaller analysed groups were inspected by t-test. Results were considered statistically different when the p value was < 0.05 .

Statistical analysis of nZVI effect on soil bacteria could not be performed due to complex and time demanding experiments which were not possible to be prepared in duplicates.



3 Results and discussion

Generally, effect of three different nanomaterials was evaluated on bacterial cultures and microbial consortia from WWTPs and soil. The first part aimed to describe unintended impact of TiO_2 and Ag NPs in WWTPs while the second part aimed to describe effect of two types of nZVI on natural soil bacteria in relation to its intended application in polluted environments.

3.1 Effect of TiO_2 and Ag NPs on bacteria from WWTPs

Nanomaterials have been increasingly used in industry, agriculture, consumer products and variety of other applications [14, 54]. Therefore, they are expected to accidentally enter the aquatic and terrestrial environments via various pathways in increasing amounts. Some studies have already described such phenomena [55, 56, 57]. Accordingly, increasing amounts of TiO_2 and Ag NPs will likely end in WWTPs where they may compromise important biodegradation processes such as nitrification and denitrification. Therefore, potential effect of TiO_2 and Ag NPs on bacterial cultures and natural bacterial communities from WWTPs is described in this section.

3.1.1 Effect of TiO_2 NPs on denitrifying bacteria

O_2 respiration by *P. denitrificans* was measured over 32 hours in three TiO_2 concentrations (0.1, 1 and 10 mg/L ; Figure 3.1).

Time course of O_2 respiration remained stable during the whole incubation time at all concentrations. Significant differences were noticed between 10 and 16 hours in 10 mg/L concentration (p value = 0.0154 in 10 hours and $p < 0.0001$ between



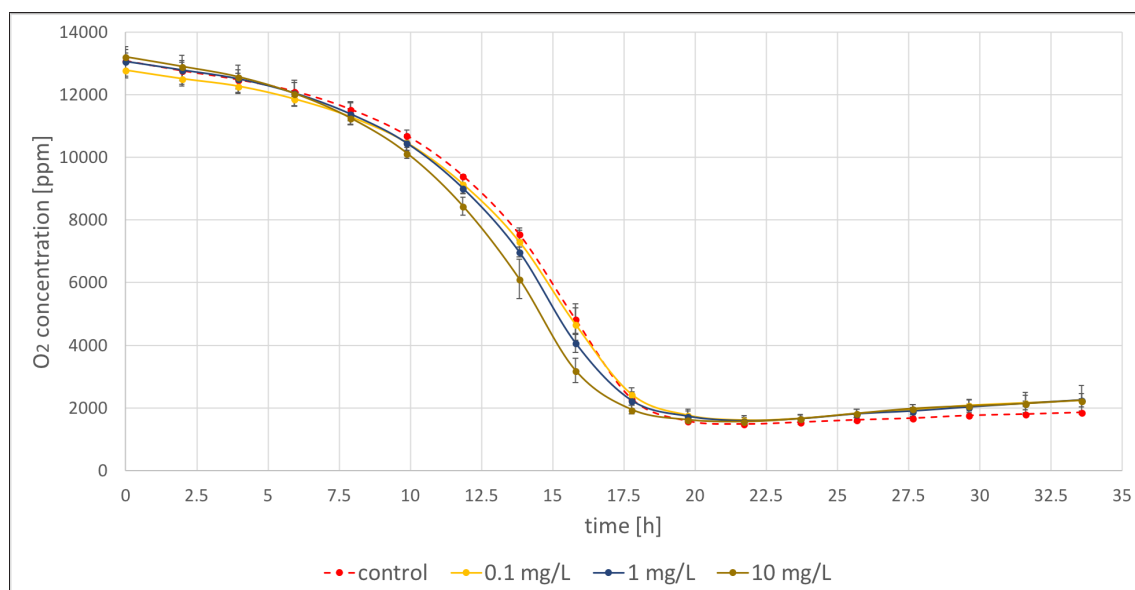


Figure 3.1: Time course of respiration of O_2 by *P. denitrificans* after exposure to various concentrations of TiO_2 NPs. Error bars represent SD of triplicate samples.

12 and 16 hours). Less significant differences were observed in the case of 1 mg/L concentration ($p = 0.0155$ and 0.0008 after 14 and 16 hours, respectively). Other concentrations and time-points showed no significant differences.

Further analysis of respiration process focused on depletion of 95% of O_2 was conducted (see Table D1). In this case, no significant difference was discovered.

Similar effect was observed with *T. linaloolentis* (see Figure 3.2). 10 mg/L concentration was significantly different between 7.1 and 16.6 hours with lowest $p < 0.0001$ between 11.9 and 14.2 hours. Statistical analysis revealed no significant variations for other concentrations.

Detailed analysis of 95% O_2 depletion due to the respiration of *T. linaloolentis* did not show any significant variations (see Table D2).

Although the concentration of 10 mg/L of TiO_2 might be high enough to somehow affect the process of O_2 respiration, the respiration was not, in fact, compromised. In addition, the time of NO highest accumulation was investigated (see Tables D3 and D4). No significant difference was observed.



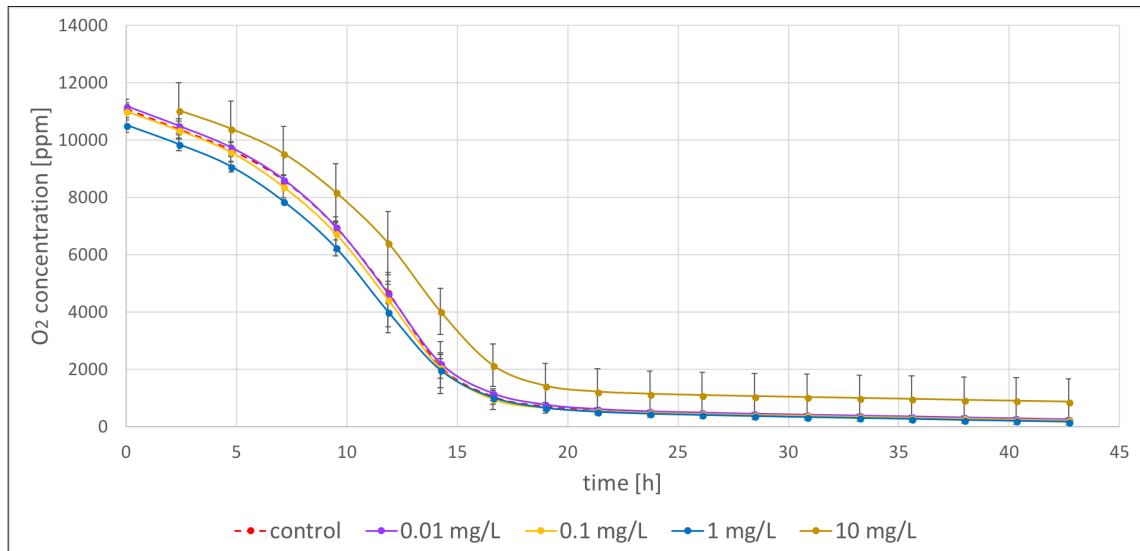


Figure 3.2: Time course of respiration of O_2 by *T. linaloolentis* after exposure to various concentrations of TiO_2 NPs. Error bars represent SD of triplicate samples.

In short, no substantial effect of TiO_2 NPs on the overall process of respiration of denitrifying bacterial cultures (*P. denitrificans* and *T. linaloolentis*) was detected. The time course of O_2 respiration revealed slight differences during the phase of significant decrease in oxygen in 10 mg/L concentration, but 95% depletion was detected in similar time with no significant variations in comparison to control.

Only a limited number of studies have been published on the topic of TiO_2 potential impact on denitrifying bacteria. Still, results of this study are in agreement with other published studies [58, 59, 60]. For instance, a report on the effect of TiO_2 NPs (0 - 10 mg/L) on the microbial communities in activated sludge have not revealed any impact [58]. Interestingly, certain concentrations of TiO_2 (5 - 60 mg/L) promoted the denitrification process in the same study. Nonetheless, this effect was not detected in my study.

Li et al. (2014) examined possible impact of TiO_2 NPs on the process of total N (nitrogen) removal from wastewater in activated sludge [59]. Low concentrations (2 - 50 mg/L) did not affect N removal, but higher concentrations (100 - 200 mg/L) induced decrease in biological N removal due to a likely inhibitory effect on the denitrification process.

Accordingly, Zheng et al. (2011) did not observe any acute effect of TiO_2 NPs (2 - 50 mg/L) on wastewater N and P (phosphorus) removal after 1 day of examination [60]. However, long-term exposure (70 days, re-supplementation of a certain amount of TiO_2 every 2 days due to likely decreasing concentration in time) of 50 mg/L resulted in significant decrease in total N removal efficiency. Further FISH analysis revealed that the abundance of nitrifying bacteria exceptionally decreased and thus led to a serious deterioration of ammonia oxidation. For this reason, nitrifying bacteria might be more sensitive to the exposure of nanoparticles.

Respiration kinetics of denitrifying bacteria after exposure to TiO_2 NPs are summarised in Figures C1, C2 and C3. No significant differences occurred.

3.1.2 Effect of Ag NPs on nitrifying bacteria

Figure 3.3 illustrates time course of O_2 respiration by *N. europaea* that was measured over 254 hours after exposure to Ag NPs (0.1 - 1000 $\mu g/L$).

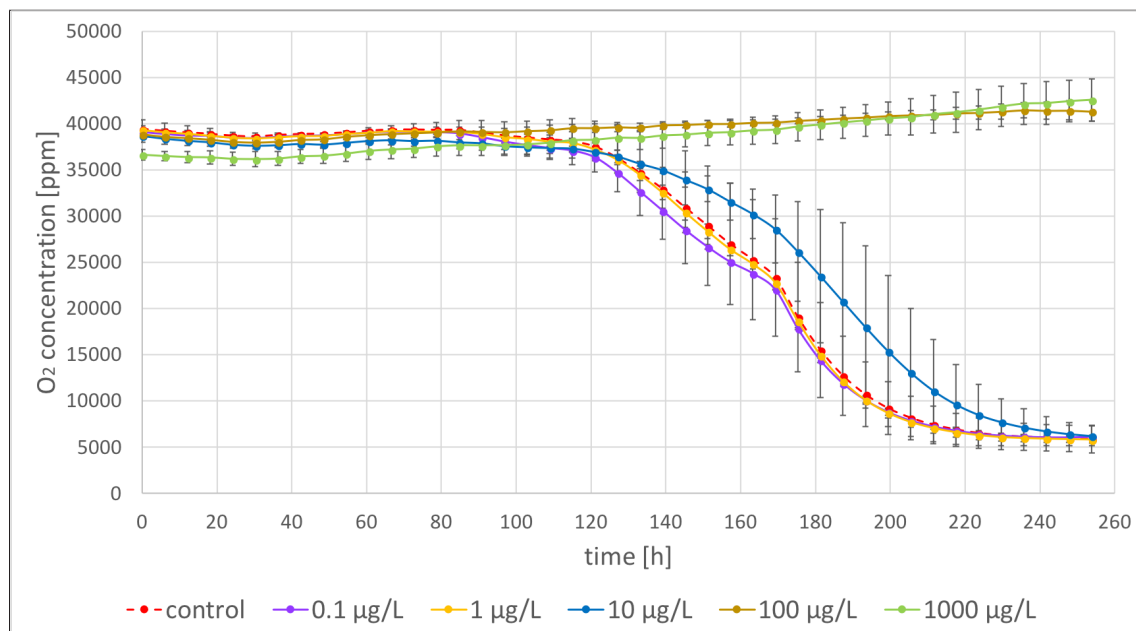


Figure 3.3: Time course of respiration of O_2 by *N. europaea* after exposure to various concentrations of Ag NPs. Error bars represent SD of duplicate samples.



Higher concentrations of *Ag* (100 and 1000 $\mu\text{g}/\text{L}$) clearly did not cause any O_2 depletion (Figure 3.3). Therefore, these doses of *Ag* NPs were likely lethal to *N. europaea*. In addition, further statistical analysis revealed that concentration of 10 $\mu\text{g}/\text{L}$ were significantly different compared to control between 169.4 and 199.5 hours ($p = 0.0341 - 0.0003$). Lower concentrations did not reveal any differences.

Analysis of times when more than 90% of O_2 was depleted (see Table D5) showed no statistical difference.

Moreover, the maximal accumulation of nitrite (NO_2^-) in time was investigated (see Table D6). 100 and 1000 $\mu\text{g}/\text{L}$ concentrations of *Ag* showed substantially lower amount of NO_2^- than other concentrations, therefore, they were not further analysed. Other concentrations revealed no significant differences.

Several studies have investigated the impact of *Ag* nanoparticles on nitrifying bacteria [20, 61, 62, 63, 64]. Inhibitory effects of *Ag* NPs on microbial growth of autotrophic nitrifying microorganisms was studied using extant respirometry and an automatic microtiter fluorescence assay [61]. It was described that 1 mg/L of *Ag* NPs had a high inhibition impact ($86 \pm 3\%$) on nitrifying microorganisms which is in a correspondence with the result of this study where the same concentration was classified as lethal. Despite this fact, dramatically lower inhibition was observed at 100 $\mu\text{g}/\text{L}$ (proximately 30%, exact numbers were not provided) than showed in my study. However, they had prepared their own NPs whereas NPs applied in this study were purchased with PVP coating and thus might less aggregate in time [65]. Bigger clusters of NPs are less harmful to cells and thus the evaluation might indicates lower inhibition. Yuan et al. (2013) evaluated toxic effect of differently-coated *Ag* nanoparticles on *N. europaea* and suggested that toxicity of *Ag* NPs is highly size and coating dependent and ought to be consistent with the released concentration of Ag^+ [66].

Similarly, Arnaout et al. (2012) investigated impacts of nanoparticle coating on

the nitrification potential of *N. europaea* [63]. They described that PVP-coated Ag NPs had the highest degree of inhibition at concentration of 20 ppm (20 mg/L). Thus, they also supported the idea that distinct Ag NPs would have different effects on *N. europaea*.

To conclude, O_2 respiration process and NO_2^- accumulation of *Nitrosomonas europaea* were negatively affected by 0.1 and 1 mg/L concentrations of PVP-coated Ag nanoparticles. Nitrification loss might occur due to ROS generation [63] and/or consequent membrane disruption [67]. No significant effect was observed in lower concentrations probably due to quick Ag passivation by sulphides [20, 68].

Although the gaseous products of nitrification are “greenhouse gases”, nitrifiers play a significant role in increasing availability of N_2 to plants in the soil and are a critical part of the WWTPs [69].

Kinetics of the respiration of *N. europaea* after exposure to Ag NPs are summarised in Figures C4 and C5. No O_2 depletion and NO_2^- accumulation were visible at the highest concentrations (100 - 1000 $\mu g/L$).

3.1.3 Effect of TiO_2 and Ag NPs on bacterial community in biofilm

In this subsection, kinetics of the respiration of bacterial community forming biofilm on LECA pellets after exposure to TiO_2 NPs, Ag NPs and their combination is discussed. All GC analysis data are summarised in Figure C6, C7 and C8.

Figure 3.4 demonstrates time course of N_2 gas production by biofilm after exposure to TiO_2 NPs. A slight variation of N_2 production of the investigated concentration was detected from 9 to 13 hours, although not significant from control sample ($p > 0.05$). Detailed statistical analysis of time when 95% of N_2 was accumulated did not reveal any significant difference (see Table D7).



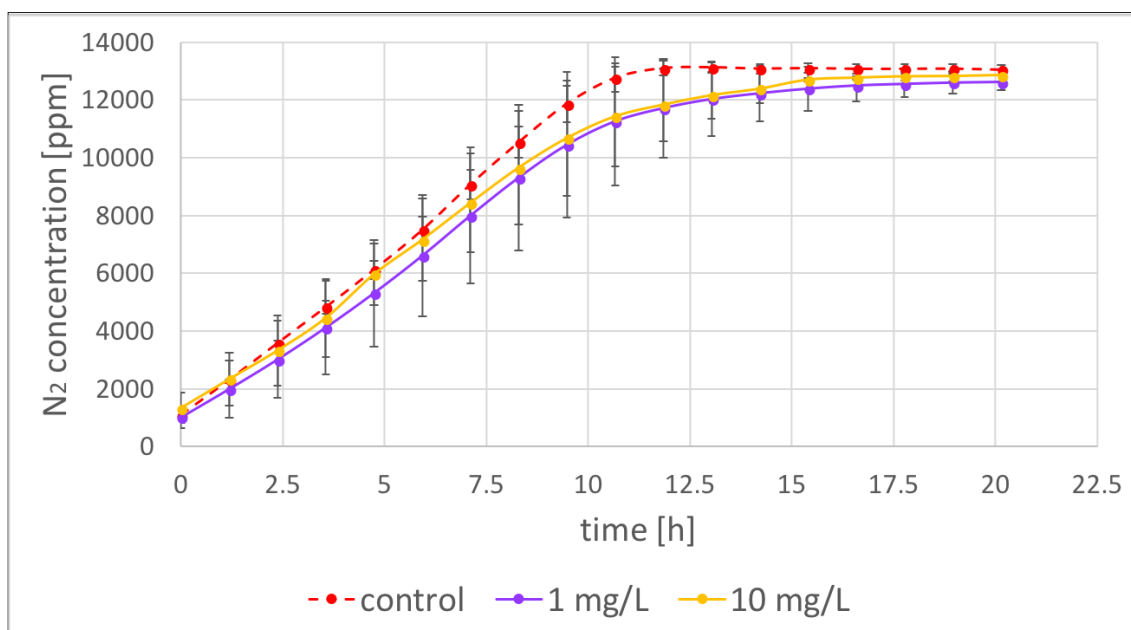


Figure 3.4: Time course of production of N_2 by bacterial consortium from biofilm after exposure to TiO_2 NPs. Error bars show SD of duplicate samples.

Similar results were observed with Ag NPs (Figure 3.5), even though some errors occurred. Unfortunately, in this case, gas leakage was observed in 1 mg/L concentration in one of the samples. Therefore, this sample was not further statistically analysed. Furthermore, significant variation in one of the samples at 0.1 mg/L concentration was detected ($p = 0.0024$). This might be again caused by a minor gas leakage, because such a phenomena was not observed in other experiments. In order to investigate 95% production of N_2 by bacterial consortium from biofilm after exposure to Ag NPs in time modified statistical analysis was conducted (see Table D10). No significant differences were observed, yet the limitations of this analysis (number of samples) must be kept in mind.

Figure 3.6 shows process of production of N_2 by investigated biofilm after exposure to combination of TiO_2 and Ag NPs.

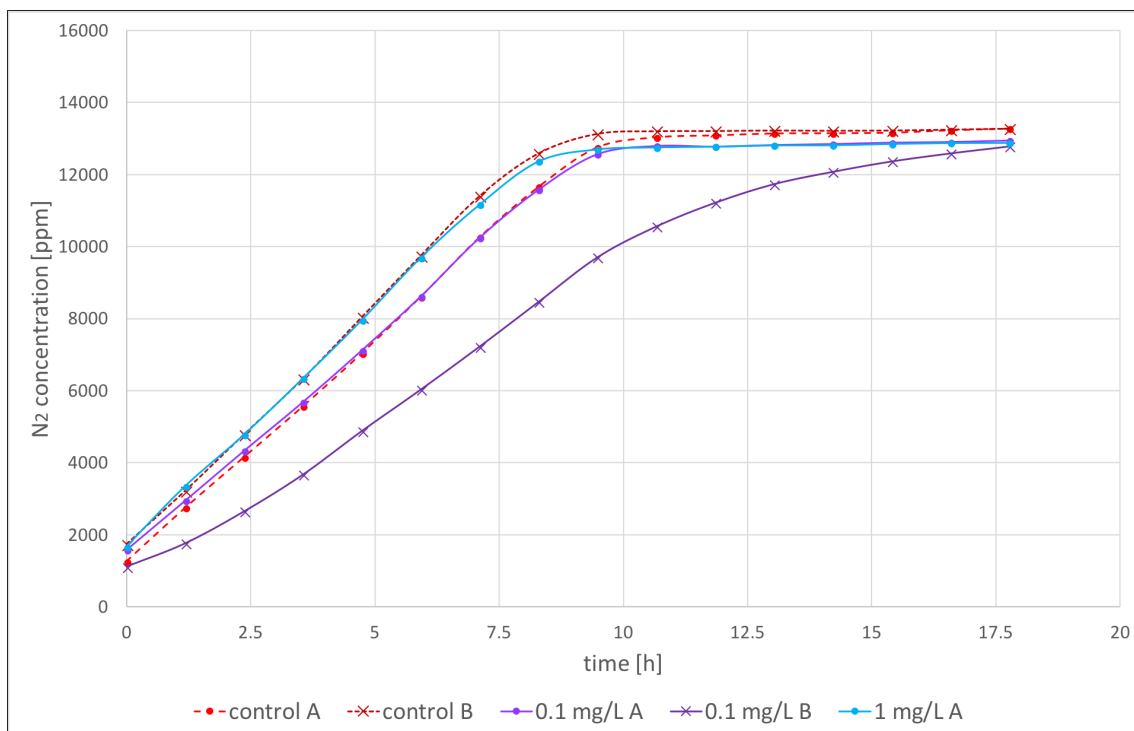


Figure 3.5: Time course of production of N_2 by bacterial consortium from biofilm after exposure to *Ag* NPs.

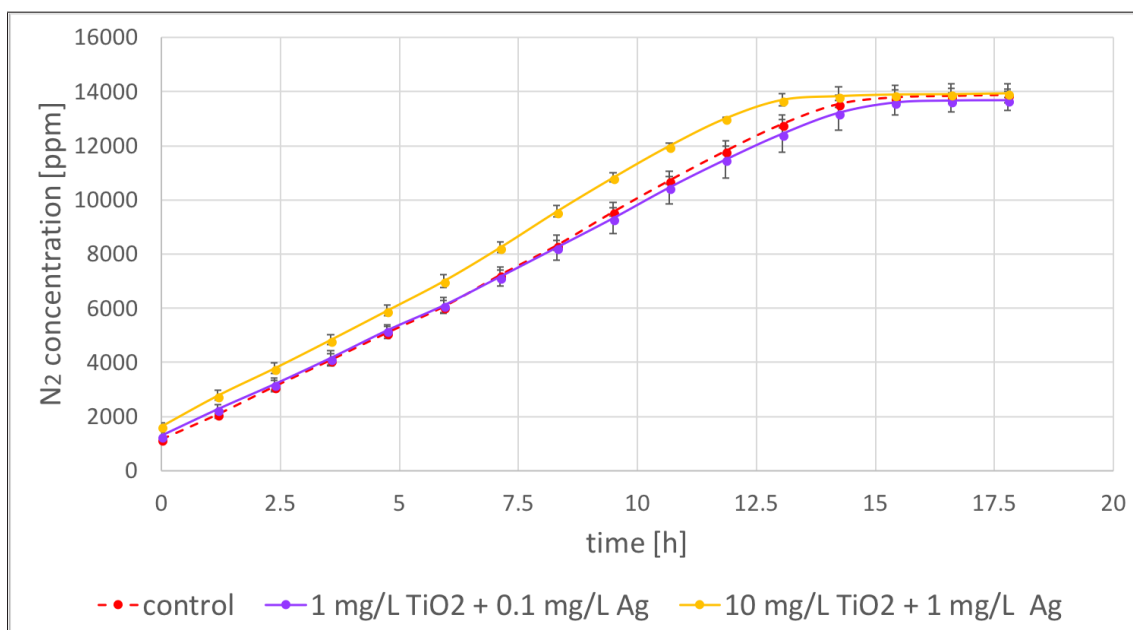


Figure 3.6: Time course of production of N_2 by bacterial consortium from biofilm after exposure to combination of TiO_2 and *Ag* NPs. Error bars are SD of duplicate samples.



Significant differences at 10 *mg/L* and 1 *mg/L* concentrations with highest *p* value (0.0002 - 0.0006) between 8.7 and 12.3 hours were observed. Detailed analysis of times when production of N_2 gas reached more than 95% did not unveil any substantial differences, however a minor delay (1.2 hours) of N_2 production with higher examined NPs concentration was detected (see Table D13).

Interestingly, time when more than 95% of N_2 was accumulated in control samples varied from one experiment to another. The same amount of LECA pellets (6 *g*) was used each time, so the volume of biofilm was similar in all samples in one experiment, but could be different in other experiment due to the different age of the biofilm and therefore the results could vary. Thus, direct comparison between these experiments was not possible.

In addition, time of the maximal accumulation of NO and NO_2^- by bacterial biofilm after exposure to various concentrations of NPs was further statistically evaluated (see Tables D8, D11 and D14 for NO analysis and Tables D9, D12 and D15 for NO_2^-). No significant differences were observed. Time of maximal accumulation of NO and NO_2^- was very similar within investigated concentrations of TiO_2 and Ag nanoparticles. It ought to be pointed out that the detection of actual concentrations of NO in time showed modest errors. In both experiments, one of the duplicates demonstrated lower amount of NO gas. In my opinion, this might be due to an insufficient stirring (problem with proper magnetic stirring on one exact spot) during the procedure. However, this error was not detected when combination of TiO_2 and Ag NPs was studied. Comparison of experiments revealed small delay of accumulation of both gases in the case of exposition to the combination of investigated NPs. Nevertheless, this effect was not significantly different.

In summary, no significant effect on the bacterial biofilm by investigated concentrations of TiO_2 and Ag NPs was detected. Despite some errors, minor impacts within each tested groups did not affect overall process of respiration.

In general, comparison between the effect of TiO_2 or Ag NPs on single bacterial

strains and bacterial biofilm revealed that the impact on biofilm was slightly lower than on single bacterial strains. Indeed, overall process of respiration on either investigated bacteria was not compromised, but minor effects occurred within some tested groups. In my opinion, the impact of NPs on bacteria from biofilm was lower due to their better protection against contaminants. Even if some of the bacterial species from the biofilm might suffer and reduce their populations, other might have replaced them and thus the global impact would have diminished. Similar conclusion was reported by Liang et al. (2010) [62]. They studied bacterial responses to a shock load of *Ag* NPs in an activated sludge and discovered that nitrification inhibition was significantly lower in activated sludge than in enriched nitrifying bacteria. They suggested that the differences could be due to factors such as bacterial concentration and NPs aggregation in the presence of extracellular polymeric substances. These substances due to its composition have high biosorption properties and thus work as a protective barrier for bacterial cells [70]. Further analysis revealed shifts in nitrifying bacterial community structure, where populations of some species drastically decreased but the overall impact was not significant.

3.1.4 Effect of TiO_2 and *Ag* NPs on bacterial community in activated sludge

Kinetics of the respiration of bacterial community located in activated sludge after exposure to TiO_2 NPs and combination of TiO_2 and *Ag* NPs is discussed in this section. Summarised data from GC are shown in Figure C9.

N_2 production by bacteria was analysed after exposure to various concentration of TiO_2 and *Ag* NPs (Figure 3.7). Control sample reached its maximal N_2 production after 11.9 hours (≈ 25000 ppm) which was well before other tested concentrations (after 21.3 hours with ≈ 38000 ppm). Unfortunately, there is no satisfactory explanation for this phenomenon, therefore it is attributed to an experimental flaw I am not able to diagnose, because all triplicate samples were very similar. This effect



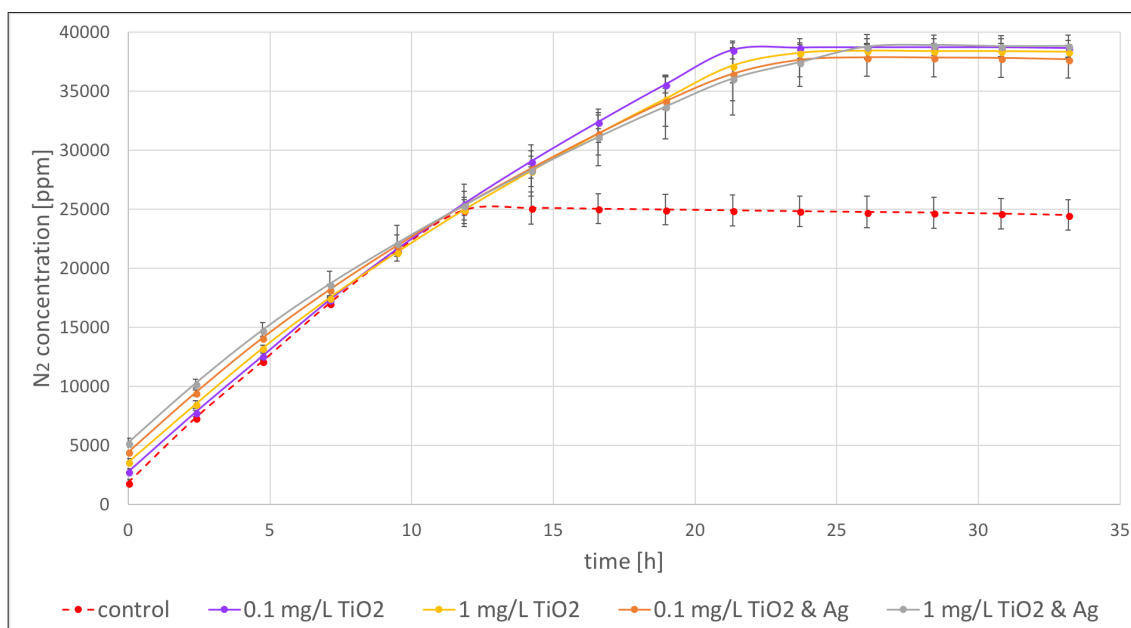


Figure 3.7: Time course of production of N_2 by bacteria community located in activated sludge after exposure to TiO_2 NPs and combination of TiO_2 and Ag NPs.

did not occur in any other experiment of this study and as far as I know, no studies have published such impact. In other experiment with biofilm (and bacterial cultures as well) the lower concentrations of TiO_2 and Ag (0.1 mg/L) were not different from control sample. For this reason, I would consider these concentrations similar to samples without NPs. Thus, this non-standard control was excluded from the evaluation.

Statistical analysis did not show any significant variations between tested concentrations. Further investigation of times when more than 95% of N_2 was produced did not reveal any significant differences, however, it seemed that with higher concentrations N_2 was produced in slower manner (see Table D16). Similar effect was observed in other experiments of this study. It was not possible to analyse NO accumulation (Figure C9) for the reason of the samples volume. First control sample was measured before the peak of maximal accumulation of NO appeared, but sampling process took few minutes and therefore the peak was not discovered in samples with higher investigated concentrations which were evaluated at last.

Several studies were published on the topic of possible effect of TiO_2 and Ag NPs on performance of bacterial community from activated sludge [58, 60, 62, 71]. Briefly, Zheng et al. (2011) revealed that the long-term exposure (70 days) of $50\text{ mg/L } TiO_2$ NPs could significantly lower the efficiency of total N removal in the activated sludge, as discussed in previous subsection (3.1.1), and caused shifts in community structure of the sequencing batch reactor (SBR) [60]. Furthermore, Li et al. (2014) described that low concentrations ($2 - 50\text{ mg/L}$) of TiO_2 NPs had no impact on total N removal from SBR during 7-day study, whereas the higher concentrations ($100 - 200\text{ mg/L}$) decreased the total N removal efficiency substantially [59]. Further investigation of an impact of TiO_2 NPs on the process of bioflocculation was evaluated [72]. Bioflocculation is a process of aggregation of microbial cells (predominantly bacteria) and pollutant particles in the wastewater [73] and it is an essential process for the activated sludge stability. It was shown that 5 ppm (5 mg/L) TiO_2 NPs did not cause significant difference in surface potentials, however, 100 ppm resulted in very strong stability which meant that long exposure of TiO_2 to the bioflocs might lead to a low deposit efficiency and afterwards to the collapse of the activated sludge treatment plant. Wang et al. (2012) studied impact of selected NPs on the ability of wastewater bacteria to biodegrade organic material via analysis of chemical O_2 demand (COD) and described that environmentally relevant loadings ($0.5 - 2\text{ mg/L}$) had negligible impact on wastewater bacteria [74]. Potential effects of sole Ag NPs are described in previous subsection (3.1.2).

To conclude, all evaluated concentrations most probably had no significant effect on N_2 production of bacterial community from activated sludge after exposure to TiO_2 and Ag NPs, however the control samples could not be included in the statistical analysis. Statistical analysis between concentrations revealed slightly bigger influence by higher concentrations. Generally speaking, TiO_2 in low concentrations (less than 5 mg/L) should not be harmful to the bacteria located in the activated sludge. Nevertheless, Ag NPs showed greater impact on the respiration kinetics at low concentrations ($0.1 - 1\text{ mg/L}$) and in high doses might be toxic to the bacte-



rial community situated in activated sludge. Moreover, both NPs undergo several transformations such as homo and heteroaggregation, degradation, sulfidation in activated sludge and therefore their original form (nano-dimension) would have entered the WWTPs in far greater amounts to cause any substantial harm. The experiments in my study illustrated the worst case scenarios where NPs suspensions could directly react with the bacterial cultures from the biofilm or the activated sludge.

3.2 Effect of nZVI on soil bacteria

The application of nanoscale zero-valent iron represents one of the most advanced technologies for environmental remediation and decontamination [6, 75]. Highly reactive materials such as nZVI have an imminent impact on natural microbial communities. These can often metabolically utilise different pollutants in soil and therefore substantially enhance the nZVI performance. Monitoring of nZVI effect on microbial communities is thus an essential part of successful evaluation of *in situ* remediation.

Furthermore, effect of nZVI on indigenous microbial communities inhabiting ordinary soil has not been sufficiently explored. This lack of knowledge might be an additional barrier for its successful commercialisation.

In this section, changes in the structure of the soil microbial community (belonging to α -*Proteobacteria*, β -*Proteobacteria*, γ -*Proteobacteria* and *Actinobacteria*) after introduction to BC-nZVI and NANOFER 25S nanoparticles inspected by FISH are described.

3.2.1 Image analysis of FISH data

Few studies have been published on the topic of nZVI influence on indigenous microbial communities using FISH method [34, 36, 76, 77].

All of them used confocal microscope for imaging process, which is far more ex-



pensive, advanced and superior to the fluorescence one. However, I was able to adjust the protocols [36, 34] and successfully operate FISH on fluorescence microscope with some shortages. Unfortunately, it was not possible to use DAPI for an additional labelling because of its extremely high brightness. On the other hand, LGC353a probe for inspection of *Firmicutes* (low G+C content) was too dimmed and faded, and thus inapplicable. This is the reason why the probe is not illustrated in Figure 3.8. In my opinion, these shortages were observed due to the application of fluorescence microscope because other research groups mentioned above faced no such problem.

FISH images are commonly analysed by a well-experienced person who counts all objects/cells manually from each image. The advantage is that the results are precise and the person can discover irregularities if some appear.

Despite the fact, from my point of view, the disadvantages outweigh advantages. If the personnel do not have enough experience or sufficiently sharp sight (to recognise the smallest objects on black background), the human-error will increase. Another problem is that the manual objects counting is immensely time-consuming. Long-time investigation could harm eyes (maximal brightness of screen is necessary for observation of small and faded objects) and ergo be dangerous.

The first solution in mind was to find software that would automatically analyse FISH images based on set requirements of investigated objects/cells by an experienced person. Unfortunately, programs or scripts such as Al-Kofahi et al. (2013) were hard to operate or simply inappropriate for this task [78].

With all these facts in mind, I decided to address dr. Lucie Svobodova, who specialises in MATLAB environment, to contribute to a creation of new script based on my expertise in FISH image analysis. This script combines the advantages of both approaches - it is fairly autonomous and swift, but more importantly, it is adequately precise in process of objects/cells recognition.



3.2.2 Comparison of BC-nZVI and NANOFER 25S impact

Both materials were developed for remediation of polluted aquifers and soils; NANOFER 25S contains higher amount of nZVI, and BC-nZVI contains biochar and less nZVI. In my opinion, NANOFER 25S was more reactive than BC-nZVI because of its initial smaller and well-dispersed particles that were produced by a specialised company. BC-nZVI suspension was dispersed manually and had a lower initial nZVI concentration due to its different structural composition (BC-nZVI 11.1% and NANOFER 25S 20% suspension).

The results of FISH analysis are shown in Figure 3.8. No substantial variations were observed in the total number of cells belonging to *Eubacteria* domain except for BC-nZVI after 16 days where lower total number of cells was observed. Nonetheless, some trends were observed within this domain.

The most striking shifts in the microbial community structure developed after 16 days. Each of examined bacterial group (α -*Proteobacteria*, β -*Proteobacteria*, γ -*Proteobacteria* and *Actinobacteria*) in control sample increase in abundance whereas in the case of BC-nZVI and NANOFER 25S, monitored bacterial groups decreased to some extent. Both materials likely caused an increase in number of other *Eubacteria* not specifically covered in this study such as *Acidithiobacillus ferrooxidans* species that are exceptionally adaptable and tolerant to harsh environmental conditions [79]. As an energy source they are oxidising iron and sulphur to support their growth and while producing ferric iron and sulphuric acid. Therefore, BC-nZVI and NANOFER 25S could donate iron to these organisms and give them a considerable advantage. The significant rise of *Fe* availability in heavy metal polluted soil treated by nZVI was observed by Fajardo et al. (2015) [77]. They analysed the *Fe* concentration associated with the most available fraction (exchangeable and linked to carbonates) and discovered that availability of *Fe* was independent on the metal contamination and, more importantly, the application of nZVI to metal-polluted soil had improved soil properties and increased *Fe* availability in the soil.



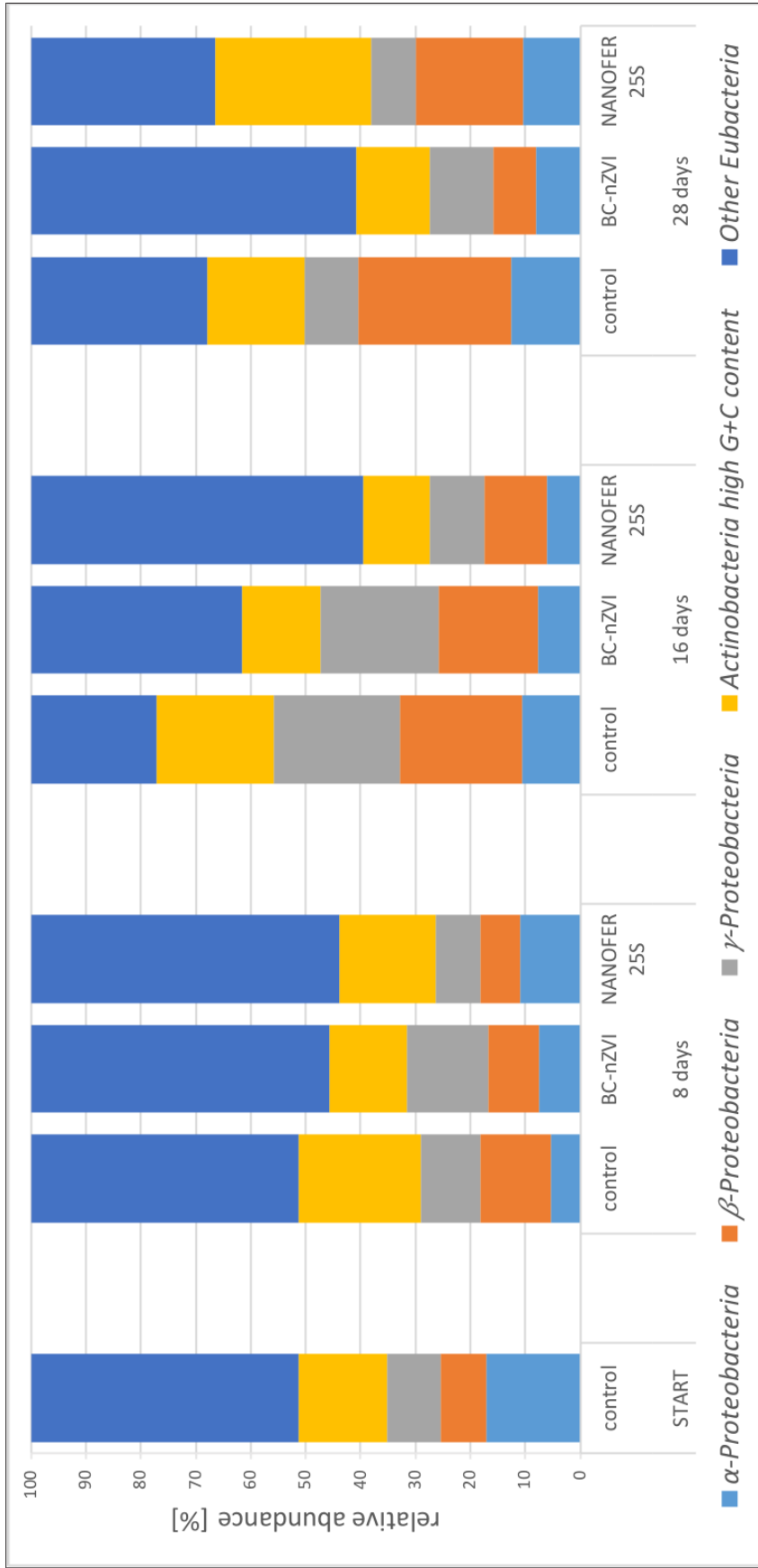


Figure 3.8: The phylogenetic microbial composition as detected by FISH.



Moreover, BC-nZVI and NANOFER 25S might induce oxidative stress in cells of bacteria that are not tolerant to higher ROS (reactive oxygen species) and thus substantially lower their abundance [80]. NANOFER 25S had higher negative impact on examined groups after 16 days which might be due to its higher reactivity. Similar results were observed by Fajardo et al. (2012), who discovered significant shifts in phylogenetic microbial composition of heavy metal (Pb and Zn) polluted soils after treatment of NANOFER 25S, providing an evidence of selective pressure on the microbial community [34]. They reported that the number of *Archaea* domain, α -*Proteobacteria* and *Firmicutes* (low G+C content) dominated, whereas the number of β -*Proteobacteria* and γ -*Proteobacteria* declined.

Interestingly, the visible impact of BC-nZVI on tested bacterial groups remained even after 28 days. BC-nZVI was partly composed of biochar which probably provided high concentration of available carbon in soil which is essential to vast majority of *Eubacteria* and therefore, it caused increase in the total number of other *Eubacteria* groups. The NANOFER 25S was very similar to control after 28 days with a slight difference in *Actinobacteria* (high G+C content). This corresponds to Sacca et al. (2014) who analysed the phylogenetic composition of microbial community of two different soils (Lufa 2.2 and 2.4) using FISH [76]. They similarly observed that NANOFER 25S had a positive effect on the number of *Actinobacteria* in soil 2.4. Nonetheless, other results showed different observation such as a negative effect of NANOFER 25S on α -*Proteobacteria* and β -*Proteobacteria* whereas in this study such effect was not observed. The differences in the phylogenetic profiles of those evaluated soils could be due to the soil matrix differences as was already reported [76].

Interesting fact is that there was no considerable impact on microbial community structure after 8 days. This might be due to a slow reaction of soil bacteria to such stimulus. Another explanation is that these organisms reacted primarily to the change of their environment rather than directly to the presence of nZVI. nZVI modifies conditions of environment such as increase in pH and decrease in PO_4^{3-}



(phosphate), NO_3^- and partly O_2 availability, to some extent [81]. However, it was reported that effects of nZVI are highly context dependent and vary notably with different soil types [82].

The buffering capacity of the soil might be crucial fact as well. Nevertheless, there was no rapid or notable change in the composition of investigated microbial community after 8 days.

Generally speaking, studies of NPs effect on bacterial communities in soil are very scarce, thus it is complicated to compare the results. Several studies have proven nZVI bactericidal effects on various soil bacteria and its possible impact on composition of microbial community [76, 82, 83]. All studies revealed that the impact of nZVI vary greatly with soil and nZVI type, indicating the importance of considering the affected matrix case by case.

Furthermore, it would be interesting to study the amount of ZVI throughout the whole experiment in order to observe a real consumption and transformation of zero-valent iron. Then, it would be possible to explain the changes in diversity in soil microbial community more precisely.

To conclude, the effect of BC-nZVI or NANOFER 25S on soil microbial community was most probably due to the changes in the soil nutrient availability or shifts in pH which are direct effect of nZVI. Nevertheless, it seems that this effect is temporary and the bacterial community structure might recover after zero-valent iron is oxidised.



4 Conclusions

This study provides a detailed analysis of possible effect of selected NPs on different bacterial strains and bacterial communities from WWTPs and soil. Each segment was thoroughly studied and results compared with current literature. In order to clarify some results, recommendations for further analysis were made. Progressive statistical tools were applied to secure a minimal error during evaluation of the results. In addition, original FISH protocol for soil samples and confocal microscopy was adjusted for the application on the fluorescence microscope. In order to enhance the process of bacterial cells enumeration, an advanced image analysis was developed and successfully applied.

TiO_2 NPs showed no significant effect on the respiration process of single strain denitrifiers *Paracoccus denitrificans* and *Thauera linaloolentis*. However, detailed analysis of O_2 respiration of *T. linaloolentis* revealed delay in the highest concentration (10 mg/L).

Ag NPs negatively affected O_2 respiration and NO_2^- accumulation of single strain nitrifier *Nitrosomonas europaea* at 0.1 and 1 mg/L. Lower concentrations did not reveal any significant effect.

TiO_2 , Ag and combination of this NPs had no substantial effect on the respiration kinetics of bacterial biofilm or activated sludge from WWTP and the overall process of respiration was not compromised.

These “worst case scenarios” experiments therefore disclose no impact of TiO_2 and Ag NPs on studied bacterial strains and communities.

Shifts in the structure of soil microbial communities after exposure to BC-nZVI or NANOFER 25S were detected by FISH. These effects occurred most likely due to changes in the soil nutrient availability or changes in pH and they seem to be temporary.



This thesis has achieved outlined goals and partly contributed to the research of *TiO₂*, *Ag* and nZVI effects on bacterial strains and communities located in WWTPs and soil.



Bibliography

1. DASTJERDI, Roya; MONTAZER, Majid; SHAHSAVAN, Shadi. A new method to stabilize nanoparticles on textile surfaces. *Colloids and Surfaces A: Physicochemical and Engineering Aspects*. 2009, vol. 345, no. 1, pp. 202–210.
2. YURANOVA, T; RINCON, AG; PULGARIN, C; LAUB, D; XANTOPOULOS, N; MATHIEU, H-J; KIWI, J. Performance and characterization of Ag–cotton and Ag/TiO₂ loaded textiles during the abatement of E. coli. *Journal of Photochemistry and Photobiology A: Chemistry*. 2006, vol. 181, no. 2, pp. 363–369.
3. MAHVI, A.H.; GHANBARIAN, M.; NASSERI, S.; KHAIRI, A. Mineralization and discoloration of textile wastewater by TiO₂ nanoparticles. *Desalination*. 2009, vol. 239, no. 1-3, pp. 309–316. Available from DOI: [10.1016/j.desal.2008.04.002](https://doi.org/10.1016/j.desal.2008.04.002).
4. GUPTA, Shipra Mital; TRIPATHI, Manoj. A review of TiO₂ nanoparticles. *Chinese Science Bulletin*. 2011, vol. 56, no. 16, pp. 1639.
5. LI, Qi; CHEN, Xijuan; ZHUANG, Jie; CHEN, Xin. Decontaminating soil organic pollutants with manufactured nanoparticles. *Environmental Science and Pollution Research*. 2016, vol. 23, no. 12, pp. 11533–11548. Available from DOI: [10.1007/s11356-016-6255-7](https://doi.org/10.1007/s11356-016-6255-7).
6. MUELLER, Nicole C; BRAUN, Jürgen; BRUNS, Johannes; ČERNÍK, Miroslav; RISSING, Peter; RICKERBY, David; NOWACK, Bernd. Application of nanoscale zero valent iron (NZVI) for groundwater remediation in Europe. *Environmental Science and Pollution Research*. 2012, vol. 19, no. 2, pp. 550–558.
7. CUNDY, Andrew B; HOPKINSON, Laurence; WHITBY, Raymond LD. Use of iron-based technologies in contaminated land and groundwater remediation: A review. *Science of the total environment*. 2008, vol. 400, no. 1-3, pp. 42–51.



8. ZHAO, Xiao; LIU, Wen; CAI, Zhengqing; HAN, Bing; QIAN, Tianwei; ZHAO, Dongye. An overview of preparation and applications of stabilized zero-valent iron nanoparticles for soil and groundwater remediation. *Water research*. 2016, vol. 100, pp. 245–266.
9. ZOU, Yidong; WANG, Xiangxue; KHAN, Ayub; WANG, Pengyi; LIU, Yunhai; ALSAEDI, Ahmed; HAYAT, Tasawar; WANG, Xiangke. Environmental remediation and application of nanoscale zero-valent iron and its composites for the removal of heavy metal ions: a review. *Environmental science & technology*. 2016, vol. 50, no. 14, pp. 7290–7304.
10. KLIMKOVA, Stepanka; CERNIK, Miroslav; LACINOVA, Lenka; FILIP, Jan; JANCIK, Dalibor; ZBORIL, Radek. Zero-valent iron nanoparticles in treatment of acid mine water from in situ uranium leaching. *Chemosphere*. 2011, vol. 82, no. 8, pp. 1178–1184.
11. NĚMEČEK, Jan; LHOTSKÝ, Ondřej; CAJTHAML, Tomáš. Nanoscale zero-valent iron application for in situ reduction of hexavalent chromium and its effects on indigenous microorganism populations. *Science of the Total Environment*. 2014, vol. 485, pp. 739–747.
12. MUN, Kyu-Shik; ALVAREZ, Sara D; CHOI, Won-Youl; SAILOR, Michael J. A stable, label-free optical interferometric biosensor based on TiO₂ nanotube arrays. *Acs Nano*. 2010, vol. 4, no. 4, pp. 2070–2076.
13. GUO, Changsheng; GE, Ming; LIU, Lu; GAO, Guandao; FENG, Yinchang; WANG, Yuqiu. Directed synthesis of mesoporous TiO₂ microspheres: catalysts and their photocatalysis for bisphenol A degradation. *Environmental science & technology*. 2009, vol. 44, no. 1, pp. 419–425.
14. LI, Xiaoyu; HE, Junhui. Synthesis of raspberry-like SiO₂–TiO₂ nanoparticles toward antireflective and self-cleaning coatings. *ACS applied materials & interfaces*. 2013, vol. 5, no. 11, pp. 5282–5290.



15. WEI, Chang; LIN, Wen Yuan; ZAINAL, Zulkarnain; WILLIAMS, Nathan E; ZHU, Kai; KRUZIC, Andrew P; SMITH, Russell L; RAJESHWAR, Krishnan. Bactericidal activity of TiO₂ photocatalyst in aqueous media: toward a solar-assisted water disinfection system. *Environmental science & technology*. 1994, vol. 28, no. 5, pp. 934–938.
16. WIJNHOFEN, SWP; DEKKERS, S; KOOI, M Jongeneel. WH (2011) «Nanomaterials in consumer products. Update of products on the European market in 2010». *National Institute for Public Health and the Environment. RIVM Report*. 2010, vol. 340370003.
17. SCHLICH, Karsten; KLAWONN, Thorsten; TERYTZE, Konstantin; HUNDRINKE, Kerstin. Hazard assessment of a silver nanoparticle in soil applied via sewage sludge. *Environmental Sciences Europe*. 2013, vol. 25, no. 1, pp. 17.
18. DOOLETTE, Casey L; MCLAUGHLIN, Michael J; KIRBY, Jason K; NAVARRO, Divina A. Bioavailability of silver and silver sulfide nanoparticles to lettuce (*Lactuca sativa*): Effect of agricultural amendments on plant uptake. *Journal of hazardous materials*. 2015, vol. 300, pp. 788–795.
19. DURENKAMP, Mark; PAWLETT, Mark; RITZ, Karl; HARRIS, Jim A; NEAL, Andrew L; MCGRATH, Steve P. Nanoparticles within WWTP sludges have minimal impact on leachate quality and soil microbial community structure and function. *Environmental Pollution*. 2016, vol. 211, pp. 399–405.
20. CHOI, Okkyoung; CLEVINGER, Thomas E.; DENG, Baolin; SURAMPALLI, Rao Y.; JR., Louis Ross; HU, Zhiqiang. Role of sulfide and ligand strength in controlling nanosilver toxicity. *Water Research*. 2009, vol. 43, no. 7, pp. 1879–1886. Available from DOI: [10.1016/j.watres.2009.01.029](https://doi.org/10.1016/j.watres.2009.01.029).
21. WANG, Peng et al. Silver Nanoparticles Entering Soils via the Wastewater–Sludge–Soil Pathway Pose Low Risk to Plants but Elevated Cl Concentrations Increase Ag Bioavailability. *Environmental Science & Technology*. 2016, vol. 50, no. 15, pp. 8274–8281. Available from DOI: [10.1021/acs.est.6b01180](https://doi.org/10.1021/acs.est.6b01180).



22. TAKHAR, Poonam; MAHANT, Sheefali. In vitro methods for nanotoxicity assessment: advantages and applications. *Arch Appl Sci Res.* 2011, vol. 3, no. 2, pp. 389–403.
23. MARQUIS, Bryce J; LOVE, Sara A; BRAUN, Katherine L; HAYNES, Christy L. Analytical methods to assess nanoparticle toxicity. *Analyst.* 2009, vol. 134, no. 3, pp. 425–439.
24. WANG, Shuguang; YU, Hongtao; WICKLIFFE, Jeffrey K. Limitation of the MTT and XTT assays for measuring cell viability due to superoxide formation induced by nano-scale TiO₂. *Toxicology in Vitro.* 2011, vol. 25, no. 8, pp. 2147–2151.
25. ZHOU, Xiaochun; XU, Weilin; LIU, Guokun; PANDA, Debashis; CHEN, Peng. Size-dependent catalytic activity and dynamics of gold nanoparticles at the single-molecule level. *Journal of the American Chemical Society.* 2009, vol. 132, no. 1, pp. 138–146.
26. HILLEGASS, Jedd M; SHUKLA, Arti; LATHROP, Sherrill A; MACPHERSON, Maximilian B; FUKAGAWA, Naomi K; MOSSMAN, Brooke T. Assessing nanotoxicity in cells in vitro. *Wiley Interdisciplinary Reviews: Nanomedicine and Nanobiotechnology.* 2010, vol. 2, no. 3, pp. 219–231.
27. SHUKLA, Ritesh K; SHARMA, Vyom; PANDEY, Alok K; SINGH, Shashi; SULTANA, Sarwat; DHAWAN, Alok. ROS-mediated genotoxicity induced by titanium dioxide nanoparticles in human epidermal cells. *Toxicology in vitro.* 2011, vol. 25, no. 1, pp. 231–241.
28. WOLFE, David. Colorimetric LDH Isoenzymes Using Prepared Agarose Film. *Laboratory Medicine.* 2016, vol. 4, no. 2, pp. 18–20.
29. ONG, Kimberly J et al. Widespread nanoparticle-assay interference: implications for nanotoxicity testing. *PLoS One.* 2014, vol. 9, no. 3, pp. e90650.



30. SHARMA, Vyom; SINGH, Poonam; PANDEY, Alok K; DHAWAN, Alok. Induction of oxidative stress, DNA damage and apoptosis in mouse liver after sub-acute oral exposure to zinc oxide nanoparticles. *Mutation Research/Genetic Toxicology and Environmental Mutagenesis*. 2012, vol. 745, no. 1, pp. 84–91.
31. FOLDBJERG, Rasmus; OLESEN, Ping; HOUGAARD, Mads; DANG, Duy Anh; HOFFMANN, Hans Jürgen; AUTRUP, Herman. PVP-coated silver nanoparticles and silver ions induce reactive oxygen species, apoptosis and necrosis in THP-1 monocytes. *Toxicology letters*. 2009, vol. 190, no. 2, pp. 156–162.
32. LEBEDOVÁ, Jana; HEDBERG, Yolanda S; ODNEVALL WALLINDER, Inger; KARLSSON, Hanna L. Size-dependent genotoxicity of silver, gold and platinum nanoparticles studied using the mini-gel comet assay and micronucleus scoring with flow cytometry. *Mutagenesis*. 2017, vol. 33, no. 1, pp. 77–85.
33. COLLINS, Andrew R. The comet assay for DNA damage and repair. *Molecular biotechnology*. 2004, vol. 26, no. 3, pp. 249.
34. FAJARDO, Carmen; ORTÍZ, LT.; RODRÍGUEZ-MEMBIBRE, ML.; NANDE, M.; LOBO, MC.; MARTIN, M. Assessing the impact of zero-valent iron (ZVI) nanotechnology on soil microbial structure and functionality: a molecular approach. *Chemosphere*. 2012, vol. 86, no. 8, pp. 802–808.
35. LOZUPONE, Catherine A; KNIGHT, Rob. Species divergence and the measurement of microbial diversity. *FEMS microbiology reviews*. 2008, vol. 32, no. 4, pp. 557–578.
36. MARTÍN, Margarita; GIBELLO, Alicia; LOBO, Carmen; NANDE, Mar; GARBI, Carlos; FAJARDO, Carmen; BARRA-CARACCILO, Anna; GRENNI, Paola; MARTÍNEZ-IÑIGO, M. José. Application of fluorescence in situ hybridization technique to detect simazine-degrading bacteria in soil samples. *Chemosphere*. 2008, vol. 71, no. 4, pp. 703–710. Available from DOI: [10.1016/j.chemosphere.2007.10.071](https://doi.org/10.1016/j.chemosphere.2007.10.071).

37. GRENNI, Paola et al. A new fluorescent oligonucleotide probe for in situ detection of s-triazine-degrading *Rhodococcus wratislaviensis* in contaminated groundwater and soil samples. *water research*. 2009, vol. 43, no. 12, pp. 2999–3008.
38. MOTER, Annette; GÖBEL, Ulf B. *Fluorescence in situ hybridization (FISH) for direct visualization of microorganisms*. Elsevier, 2000.
39. MOLSTAD, Lars; DÖRSCH, Peter; BAKKEN, Lars R. Robotized incubation system for monitoring gases (O₂, NO, N₂O N₂) in denitrifying cultures. *Journal of Microbiological Methods*. 2007, vol. 71, no. 3, pp. 202–211. Available from DOI: [10.1016/j.mimet.2007.08.011](https://doi.org/10.1016/j.mimet.2007.08.011).
40. PASCALE, Raffaella; CAIVANO, Marianna; BUCHICCHIO, Alessandro; MANCINI, Ignazio M; BIANCO, Giuliana; CANIANI, Donatella. Validation of an analytical method for simultaneous high-precision measurements of greenhouse gas emissions from wastewater treatment plants using a gas chromatography-barrier discharge detector system. *Journal of Chromatography a*. 2017, vol. 1480, pp. 62–69.
41. WEIDINGER, Adelheid; KOZLOV, Andrey V. Biological activities of reactive oxygen and nitrogen species: oxidative stress versus signal transduction. *Biomolecules*. 2015, vol. 5, no. 2, pp. 472–484.
42. BÄUMLER, Andreas J; SPERANDIO, Vanessa. Interactions between the microbiota and pathogenic bacteria in the gut. *Nature*. 2016, vol. 535, no. 7610, pp. 85.
43. LU, Yuan; SLOMBERG, Danielle L; SCHOENFISCH, Mark H. Nitric oxide-releasing chitosan oligosaccharides as antibacterial agents. *Biomaterials*. 2014, vol. 35, no. 5, pp. 1716–1724.
44. KELLER, Arturo A; GARNER, Kendra; MILLER, Robert J; LENIHAN, Hunter S. Toxicity of nano-zero valent iron to freshwater and marine organisms. *PloS one*. 2012, vol. 7, no. 8, pp. e43983.



45. BAKER, Simon C; FERGUSON, Stuart J; LUDWIG, Bernd; PAGE, M Dudley; RICHTER, Oliver-Matthias H; SPANNING, Rob JM van. Molecular Genetics of the Genus *Paracoccus*: Metabolically Versatile Bacteria with Bioenergetic Flexibility. *Microbiology and Molecular Biology Reviews*. 1998, vol. 62, no. 4, pp. 1046–1078.
46. SISTROM, W. R. The Kinetics of the Synthesis of Photopigments in *Rhodospseudomonas spheroides*. *Journal of General Microbiology*. 1962, vol. 28, no. 4, pp. 607–616. Available from DOI: [10.1099/00221287-28-4-607](https://doi.org/10.1099/00221287-28-4-607).
47. LIU, Binbin; MAO, Yuejian; BERGAUST, Linda; BAKKEN, Lars R.; FROSTEGÅRD, Åsa. Strains in the genus *Thauera* exhibit remarkably different denitrification regulatory phenotypes. *Environmental Microbiology*. 2013, pp. n/a–n/a. Available from DOI: [10.1111/1462-2920.12142](https://doi.org/10.1111/1462-2920.12142).
48. MAO, Yuejian; BAKKEN, Lars R; ZHAO, Liping; FROSTEGÅRD, Åsa. Functional robustness and gene pools of a wastewater nitrification reactor: comparison of dispersed and intact biofilms when stressed by low oxygen and low pH. *FEMS microbiology ecology*. 2008, vol. 66, no. 1, pp. 167–180.
49. MOLSTAD, Lars; DÖRSCH, Peter; BAKKEN, Lars R. Improved robotized incubation system for gas kinetics in batch cultures. 2016. Available from DOI: [10.13140/RG.2.2.30688.07680](https://doi.org/10.13140/RG.2.2.30688.07680).
50. COX, Robert D. Determination of nitrate and nitrite at the parts per billion level by chemiluminescence. *Analytical Chemistry*. 1980, vol. 52, no. 2, pp. 332–335.
51. BEYENAL, H; LEWANDOWSKI, Z. *Fundamentals of biofilm research*. CRC, 2007.
52. WU, Qiang; MERCHANT, Fatima; CASTLEMAN, Kenneth. *Microscope image processing*. Academic press, 2010.
53. GONZALEZ, Rafael C; WOODS, Richard E. *Digital image processing*. Upper Saddle River, NJ: Prentice Hall, 2012.



54. GOTTSCHALK, Fadri; SONDERER, Tobias; SCHOLZ, Roland W; NOWACK, Bernd. Modeled environmental concentrations of engineered nanomaterials (TiO₂, ZnO, Ag, CNT, fullerenes) for different regions. *Environmental science & technology*. 2009, vol. 43, no. 24, pp. 9216–9222.
55. KÄGI, Ralf et al. Synthetic TiO₂ nanoparticle emission from exterior facades into the aquatic environment. *Environmental pollution*. 2008, vol. 156, no. 2, pp. 233–239.
56. BOTTA, Céline; LABILLE, Jérôme; AUFFAN, Mélanie; BORSCHNECK, Daniel; MICHE, Hélène; CABIÉ, Martiane; MASIION, Armand; ROSE, Jérôme; BOTTERO, Jean-Yves. TiO₂-based nanoparticles released in water from commercialized sunscreens in a life-cycle perspective: Structures and quantities. *Environmental Pollution*. 2011, vol. 159, no. 6, pp. 1543–1550.
57. SCHAUMANN, Gabriele E et al. Understanding the fate and biological effects of Ag-and TiO₂-nanoparticles in the environment: The quest for advanced analytics and interdisciplinary concepts. *Science of the Total Environment*. 2015, vol. 535, pp. 3–19.
58. LI, Zhiwei et al. Long-term impacts of titanium dioxide nanoparticles (TiO₂ NPs) on performance and microbial community of activated sludge. *Bioresource technology*. 2017, vol. 238, pp. 361–368.
59. LI, Dapeng; CUI, Fuyi; ZHAO, Zhiwei; LIU, Dongmei; XU, Yongpeng; LI, Huiting; YANG, Xiaonan. The impact of titanium dioxide nanoparticles on biological nitrogen removal from wastewater and bacterial community shifts in activated sludge. *Biodegradation*. 2014, vol. 25, no. 2, pp. 167–177.
60. ZHENG, Xiong; CHEN, Yinguang; WU, Rui. Long-term effects of titanium dioxide nanoparticles on nitrogen and phosphorus removal from wastewater and bacterial community shift in activated sludge. *Environmental science & technology*. 2011, vol. 45, no. 17, pp. 7284–7290.



61. CHOI, Okkyoung; DENG, Kathy Kanjun; KIM, Nam-Jung; ROSS JR, Louis; SURAMPALLI, Rao Y; HU, Zhiqiang. The inhibitory effects of silver nanoparticles, silver ions, and silver chloride colloids on microbial growth. *Water research*. 2008, vol. 42, no. 12, pp. 3066–3074.
62. LIANG, Zhihua; DAS, Atreyee; HU, Zhiqiang. Bacterial response to a shock load of nanosilver in an activated sludge treatment system. *Water Research*. 2010, vol. 44, no. 18, pp. 5432–5438.
63. ARNAOUT, Christina L; GUNSCH, Claudia K. Impacts of silver nanoparticle coating on the nitrification potential of *Nitrosomonas europaea*. *Environmental science & technology*. 2012, vol. 46, no. 10, pp. 5387–5395.
64. RADNIECKI, Tyler S; STANKUS, Dylan P; NEIGH, Arianne; NASON, Jeffrey A; SEMPRINI, Lewis. Influence of liberated silver from silver nanoparticles on nitrification inhibition of *Nitrosomonas europaea*. *Chemosphere*. 2011, vol. 85, no. 1, pp. 43–49.
65. ROH, Jinkyu; UMH, Ha Nee; SIM, Jaehoon; PARK, Sumin; YI, Jongheop; KIM, Younghun. Dispersion stability of citrate-and PVP-AgNPs in biological media for cytotoxicity test. *Korean Journal of Chemical Engineering*. 2013, vol. 30, no. 3, pp. 671–674.
66. YUAN, Zhihua; LI, Jiangwei; CUI, Li; XU, Bin; ZHANG, Hongwu; YU, Chang-Ping. Interaction of silver nanoparticles with pure nitrifying bacteria. *Chemosphere*. 2013, vol. 90, no. 4, pp. 1404–1411.
67. SU, Hong-Lin; CHOU, Chih-Cheng; HUNG, Da-Jen; LIN, Siou-Hong; PAO, I-Chuan; LIN, Jun-Hong; HUANG, Fang-Liang; DONG, Rui-Xuan; LIN, Jiang-Jen. The disruption of bacterial membrane integrity through ROS generation induced by nanohybrids of silver and clay. *Biomaterials*. 2009, vol. 30, no. 30, pp. 5979–5987.
68. KUMAR, Vineet; DASGUPTA, Nandita; RANJAN, Shivendu. *Environmental Toxicity of Nanomaterials*. CRC Press, 2018.



69. CHAIN, Patrick et al. Complete genome sequence of the ammonia-oxidizing bacterium and obligate chemolithoautotroph *Nitrosomonas europaea*. *Journal of bacteriology*. 2003, vol. 185, no. 9, pp. 2759–2773.
70. COMTE, Sophie; GUIBAUD, Gilles; BAUDU, Michel. Biosorption properties of extracellular polymeric substances (EPS) resulting from activated sludge according to their type: soluble or bound. *Process Biochemistry*. 2006, vol. 41, no. 4, pp. 815–823.
71. ZHANG, Chiqian; LIANG, Zhihua; HU, Zhiqiang. Bacterial response to a continuous long-term exposure of silver nanoparticles at sub-ppm silver concentrations in a membrane bioreactor activated sludge system. *Water research*. 2014, vol. 50, pp. 350–358.
72. YANG, Xiaonan; CUI, Fuyi; GUO, Xiaochun; LI, Dapeng. Effects of nanosized titanium dioxide on the physicochemical stability of activated sludge flocs using the thermodynamic approach and Kelvin probe force microscopy. *Water research*. 2013, vol. 47, no. 12, pp. 3947–3958.
73. WILÉN, Britt-Marie; ONUKI, Motoharu; HERMANSSON, Malte; LUMLEY, Doug; MINO, Takashi. Microbial community structure in activated sludge floc analysed by fluorescence in situ hybridization and its relation to floc stability. *Water research*. 2008, vol. 42, no. 8-9, pp. 2300–2308.
74. WANG, Yifei; WESTERHOFF, Paul; HRISTOVSKI, Kiril D. Fate and biological effects of silver, titanium dioxide, and C60 (fullerene) nanomaterials during simulated wastewater treatment processes. *Journal of Hazardous Materials*. 2012, vol. 201, pp. 16–22.
75. FU, Fenglian; DIONYSIOU, Dionysios D; LIU, Hong. The use of zero-valent iron for groundwater remediation and wastewater treatment: a review. *Journal of hazardous materials*. 2014, vol. 267, pp. 194–205.
76. SACCÀ, Maria Ludovica; FAJARDO, Carmen; COSTA, Gonzalo; LOBO, Carmen; NANDE, Mar; MARTIN, Margarita. Integrating classical and molecular



- approaches to evaluate the impact of nanosized zero-valent iron (nZVI) on soil organisms. *Chemosphere*. 2014, vol. 104, pp. 184–189.
77. FAJARDO, Carmen; GIL-DÍAZ, Maria; COSTA, Gonzalo; ALONSO, J.; GUERRERO, AM; NANDE, Mar; LOBO, Carmen; MARTÍN, Margarita. Residual impact of aged nZVI on heavy metal-polluted soils. *Science of the Total Environment*. 2015, vol. 535, pp. 79–84.
 78. AL-KOFAHI, Yousef; PADFIELD, Dirk; SEPPO, Antti. An automated algorithm for cell-level FISH dot counting. In: *Medical Imaging 2013: Image Processing*. 2013, vol. 8669, p. 866903.
 79. KUMAR, Naresh; MILLOT, Romain; BATTAGLIA-BRUNET, Fabienne; OMOREGIE, Enoma; CHAURAND, Perrine; BORSCHNECK, Daniel; BASTIAENS, Leen; ROSE, Jérôme. Microbial and mineral evolution in zero valent iron-based permeable reactive barriers during long-term operations. *Environmental Science and Pollution Research*. 2016, vol. 23, no. 6, pp. 5960–5968.
 80. ŠEVČU, Alena; EL-TEMSAH, Yehia S; JONER, Erik J; ČERNÍK, Miroslav. Oxidative stress induced in microorganisms by zero-valent iron nanoparticles. *Microbes and Environments*. 2011, vol. 26, no. 4, pp. 271–281.
 81. SUN, Yuan-Pang; LI, Xiao-qin; CAO, Jiasheng; ZHANG, Wei-xian; WANG, H Paul. Characterization of zero-valent iron nanoparticles. *Advances in colloid and interface science*. 2006, vol. 120, no. 1-3, pp. 47–56.
 82. PAWLETT, Mark; RITZ, Karl; DOREY, Robert A; ROCKS, Sophie; RAMSDEN, Jeremy; HARRIS, Jim A. The impact of zero-valent iron nanoparticles upon soil microbial communities is context dependent. *Environmental Science and Pollution Research*. 2013, vol. 20, no. 2, pp. 1041–1049.
 83. NOGUEIRA, Verónica et al. Impact of organic and inorganic nanomaterials in the soil microbial community structure. *Science of the total environment*. 2012, vol. 424, pp. 344–350.

Appendix A

Table A1: Sistrom's medium

Chemical	[g/L]
K_2HPO_4	3.48 g
$(NH_4)_2SO_4$	0.50 g
succinic acid	4.0 g
L-glutamin acid	0.10 g
L-aspartic acid	0.04 g
$NaCl$	0.50 g
nitrilotriacetic acid	0.20 g
$MgSO_4 * 7H_2O$	0.30 g
$CaCl_2 * 2H_2O$	0.033 g



Table A2: Trace elements and vitamins solution for *Paracoccus*'s medium

Chemical	[g/L]
EDTA	1.765 mg
$ZnSO_4 * 7H_2O$	10.95 mg
$FeSO_4 * 7H_2O$	5 mg
$MnSO_4 * H_2O$	1.54 mg
$CuSO_4 * 5H_2O$	0.392 mg
$Co(NO_3)_2 * 6H_2O$	0.248 mg
H_3BO_3	0.114 mg
nicotinic acid	1.0 mg
thiamine HCl	0.5 mg
biotin	0.010 mg

Table A3: Thauera's medium

Chemical	[g/L]
NH_4Cl	0.45 g
K_2SO_4	0.05 g
$MgCl_2 * 6H_2O$	0.1 g
$CaCl_2 * 2H_2O$	0.025 g
$NaHCO_3$	0.04 g
CH_3COONa	0.2 g
peptone	0.5 g
meat extract	0.3 g
1 M NaH_2PO_4	15.5 mL
1 M Na_2HPO_4	84.5 mL



Table A4: Basal salts medium

Chemical	[g/L]
<i>NaCl</i>	1.0 g
<i>MgCl₂ * 6H₂O</i>	0.4 g
<i>CaCl₂ * 2H₂O</i>	0.1 g
<i>KH₂PO₄</i>	0.2 g
<i>KCl</i>	0.5 g
1 M <i>NaHCO₃</i>	2.0 mL
7.5 mM <i>FeNaEDTA</i>	1.0 mL
1 M <i>NH₄Cl</i>	0.5 mL

Table A5: Modified trace elements solution for *Nitrosomonas*'s medium

Chemical	[g/L]
<i>H₃BO₃</i>	30 mg
<i>MnCl₂ * 4H₂O</i>	100 mg
<i>CoCl₂ * 6H₂O</i>	190 mg
<i>NiCl₂ * 6H₂O</i>	24 mg
<i>CuCl₂ * 2H₂O</i>	2.0 mg
<i>ZnSO₄ * 7H₂O</i>	144 mg
<i>Na₂MoO₄ * 6H₂O</i>	36 mg
12.5 M <i>HCl</i>	8.0 mL



Table A6: The main characteristics of the soil.

standard soil type no.	2.3
batch no. (SP=stored; F=field fresh)	SP 2.3 08/2015
sampling date	18/02/2015
organic carbon in % <i>C</i>	0.67 ± 0.03
nitrogen in % <i>N</i>	0.08 ± 0.01
pH value (0.01 M <i>CaCl</i> ₂)	5.9 ± 0.6
cation exchange capacity (meq/100g)	7.6 ± 0.8
soil type	sandy loam
maximum water holding capacity (g/100g)	35.6 ± 1.4
weight per volume (g/1000 mL)	1310 ± 43

Table A7: Synthetic wastewater solution

Chemical	[mg/L]
<i>CaCl</i> ₂	127.5
<i>NaHCO</i> ₃	210.0
<i>NaCl</i>	200.0
<i>NH</i> ₄ <i>Cl</i>	100.0
<i>K</i> ₂ <i>HPO</i> ₄	50.0
Dry milk	300.0
Potato starch	60.0

Appendix B

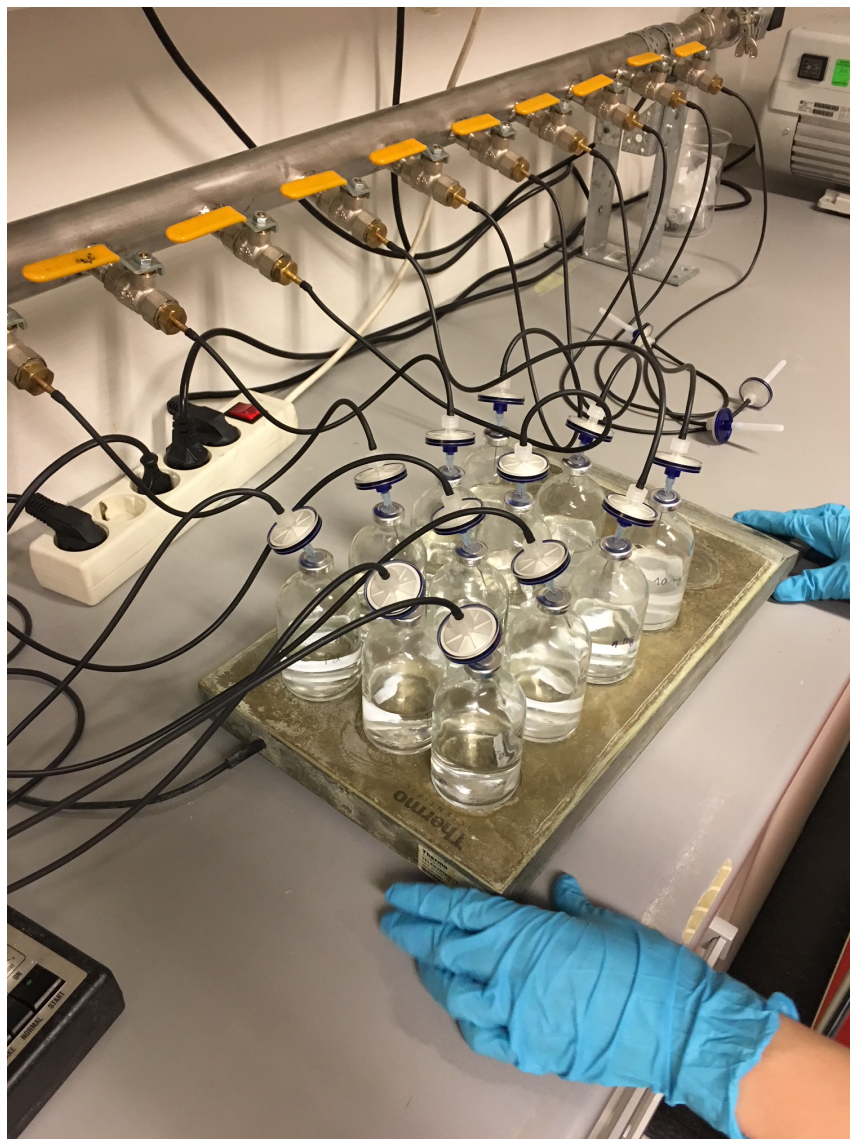


Figure B1: Evacuation and a helium-filling semi-automated system for GC analysis.





Figure B2: Stainless steel gas-tight reactors for biofilm testing.

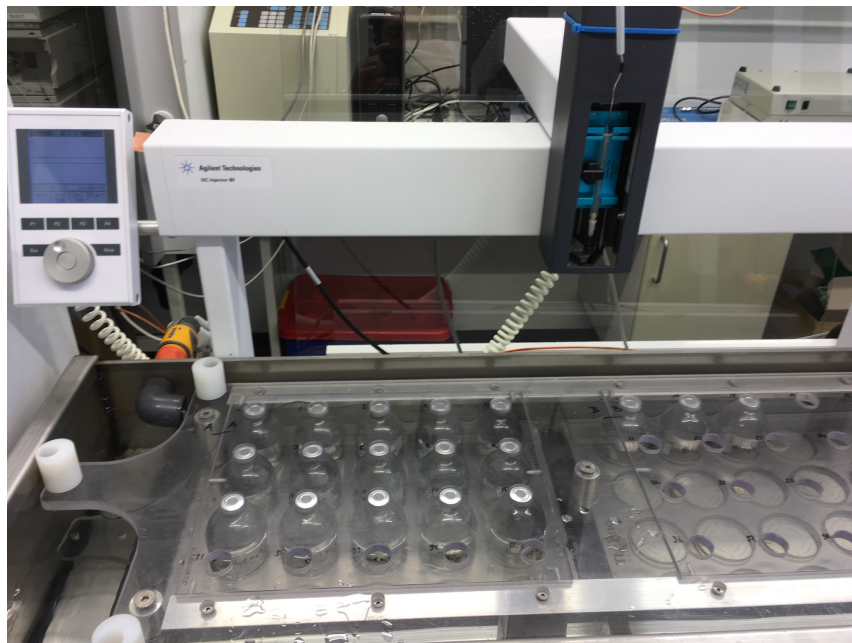


Figure B3: Improved version of robotised gas analysis system [39].

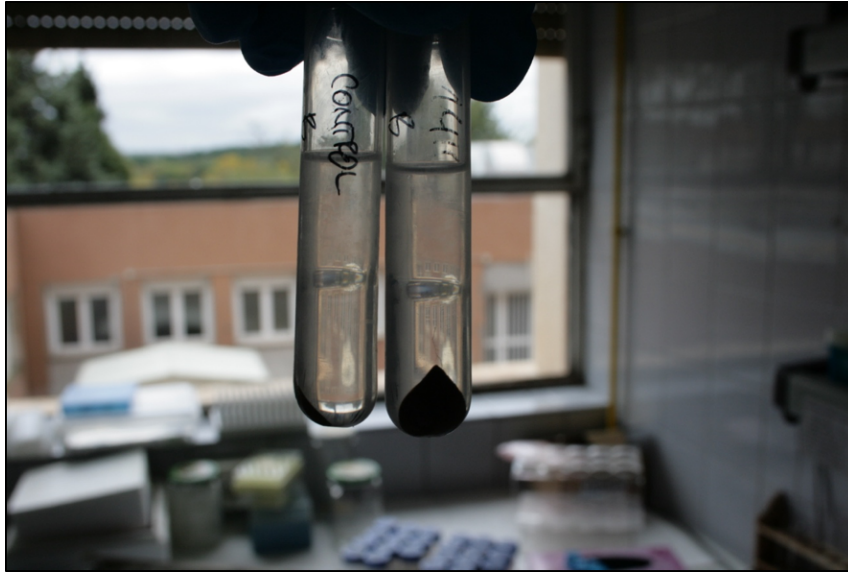


Figure B4: Demonstration of the intermediate phase that consisted of 400 μL of the cell layer.

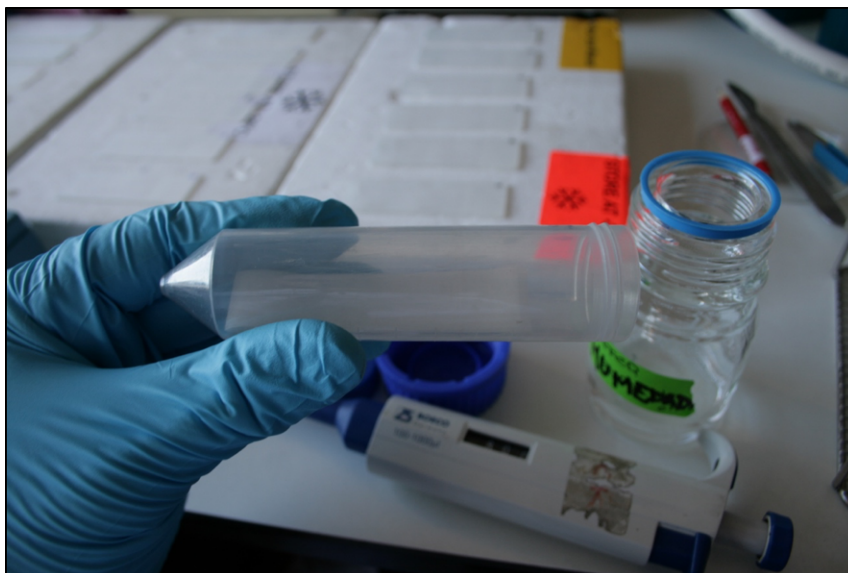


Figure B5: The falcon tube with the filtration paper ready for the filter entry.



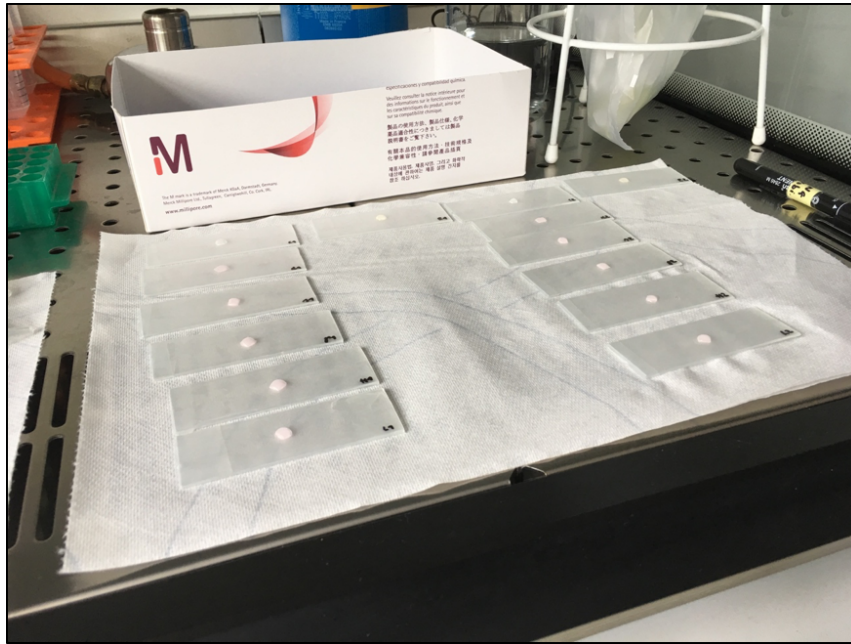


Figure B6: Filters prepared for hybridisation.

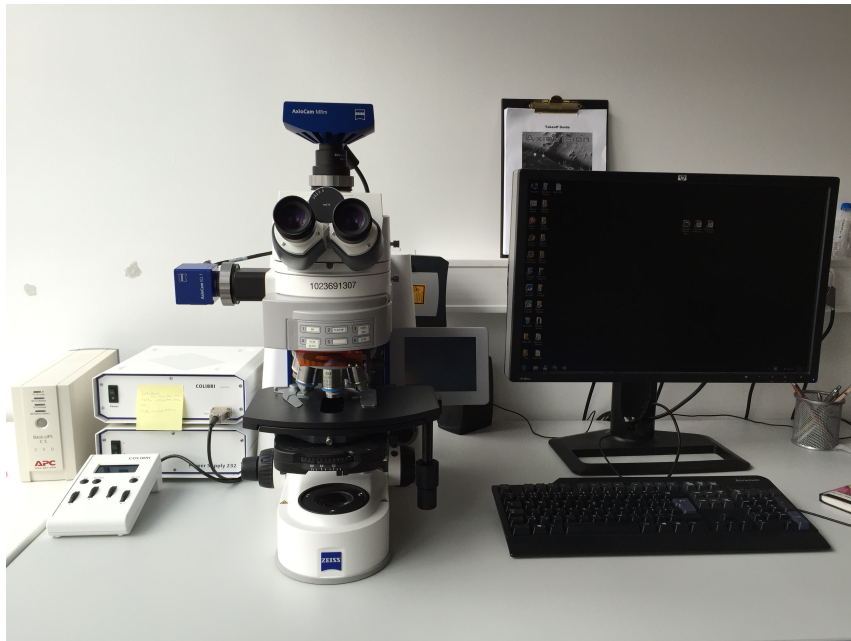


Figure B7: Fluorescence microscope (Axiomager, ZEISS, Germany).



Appendix C



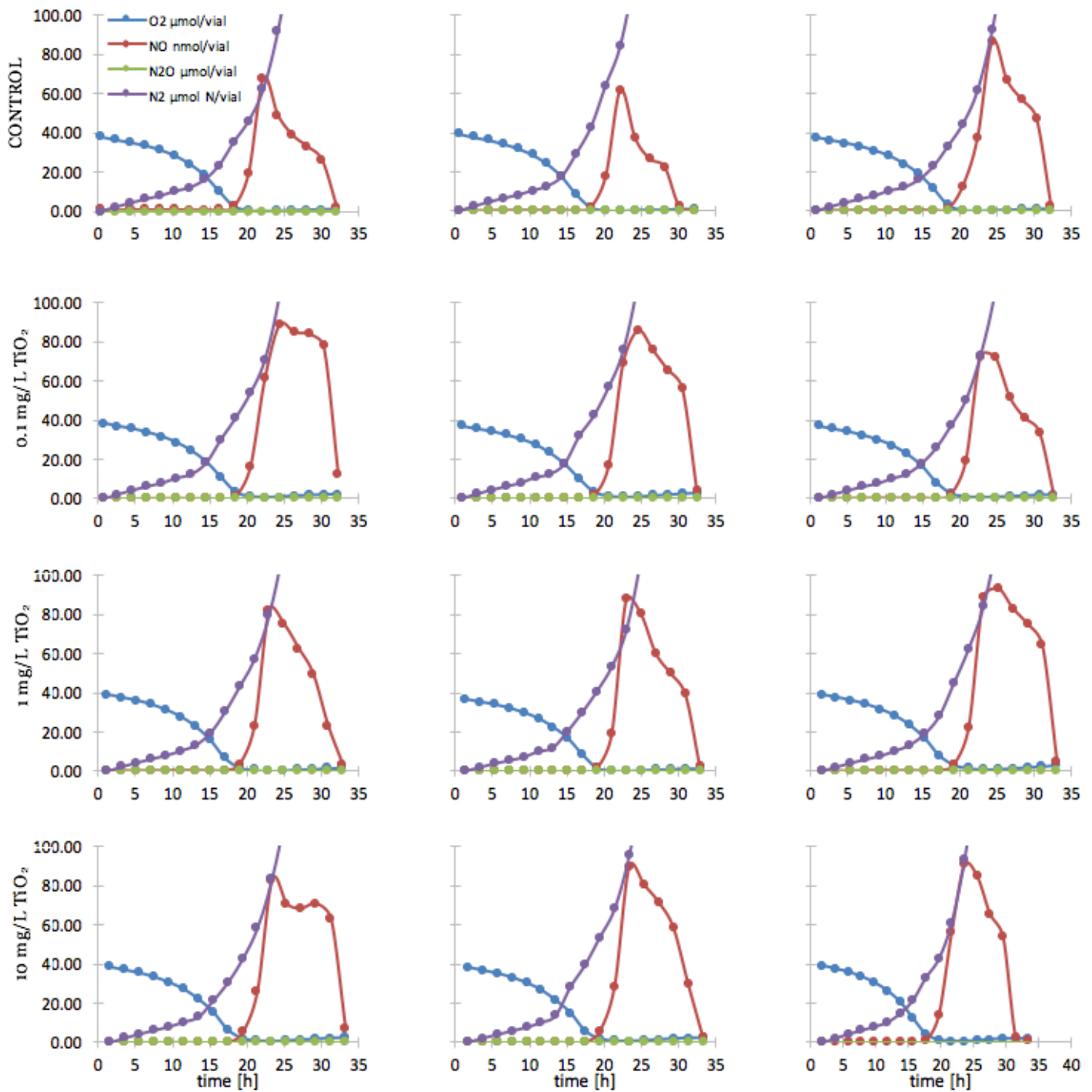


Figure C1: Kinetics of the respiration of *P. denitrificans* after exposure to TiO_2 NPs. Each plot represents one sample.



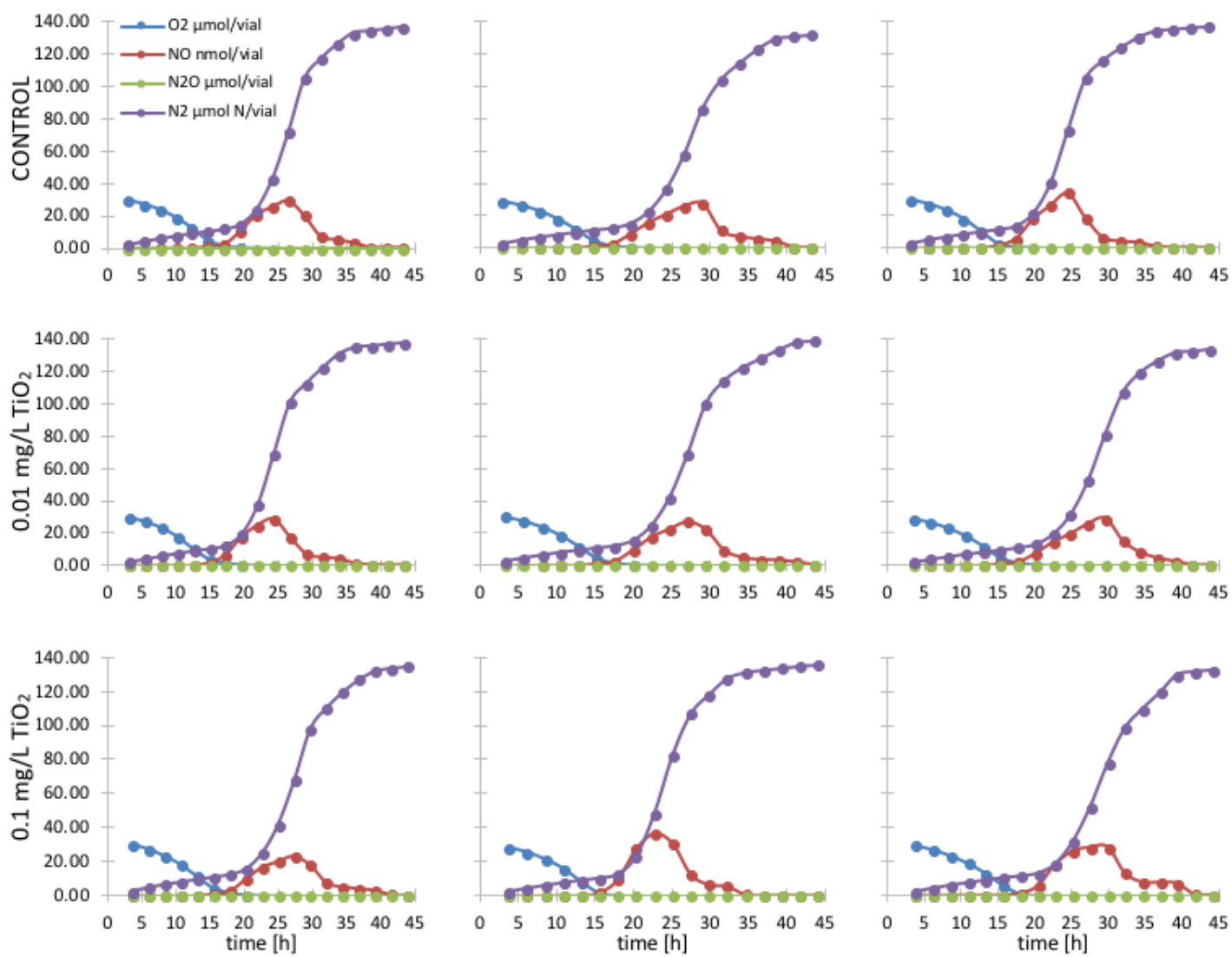


Figure C2: Kinetics of the respiration of *T. linaloolentis* after exposure to TiO_2 NPs with concentration of 0.01 and 0.1 mg/L. Each plot represents one sample.

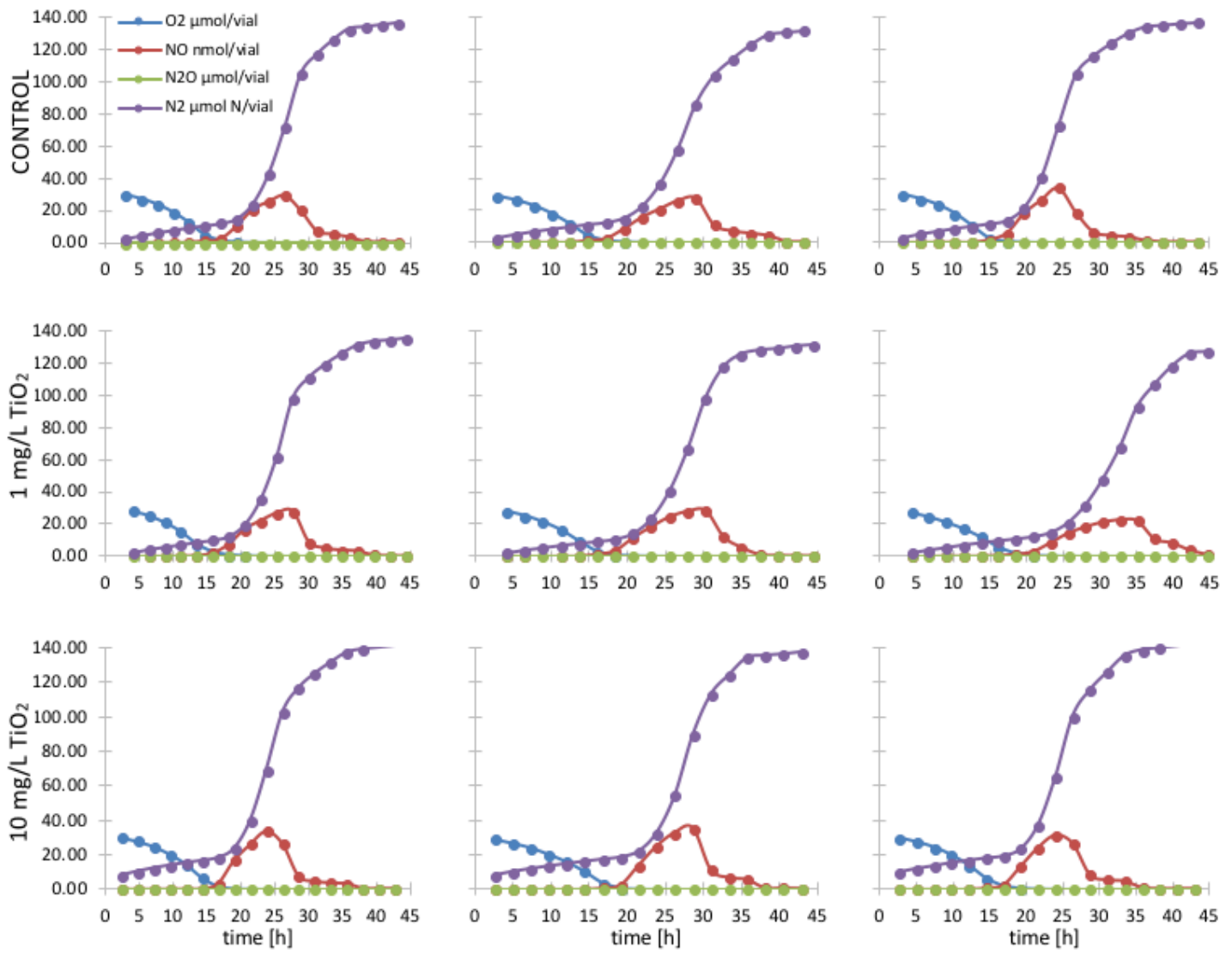


Figure C3: Kinetics of the respiration of *T. linaloolentis* after exposure to TiO_2 NPs with concentration of 1 and 10 mg/L. Each plot represents one sample.



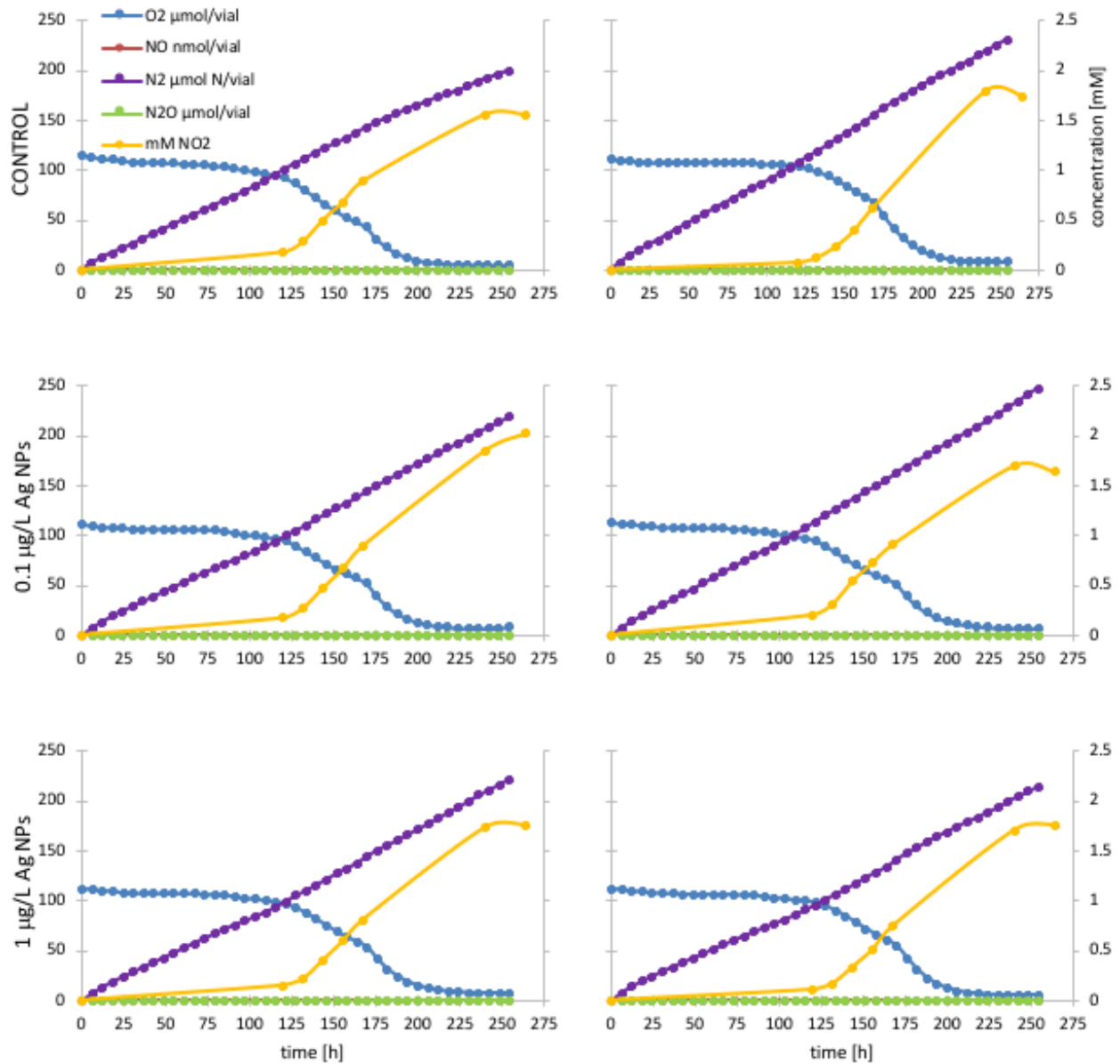


Figure C4: Kinetics of the respiration of *N. europaea* after exposure to Ag NPs with concentration of 0.1 and 1 µg/L. Each plot represents one sample.



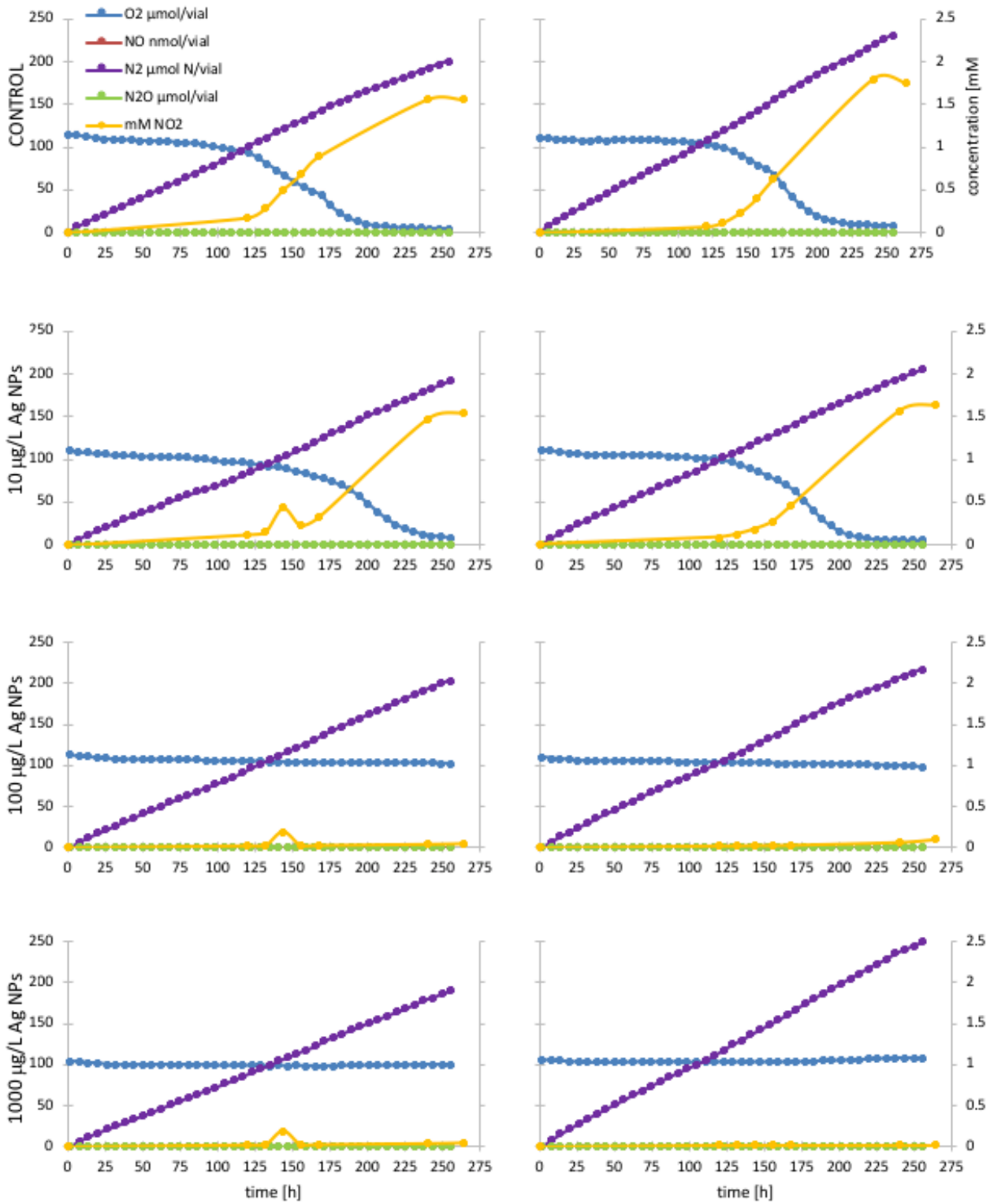


Figure C5: Kinetics of the respiration of *N. europaea* after exposure to *Ag* NPs with concentration of 10 and 1000 $\mu\text{g/L}$. Each plot represents one sample.



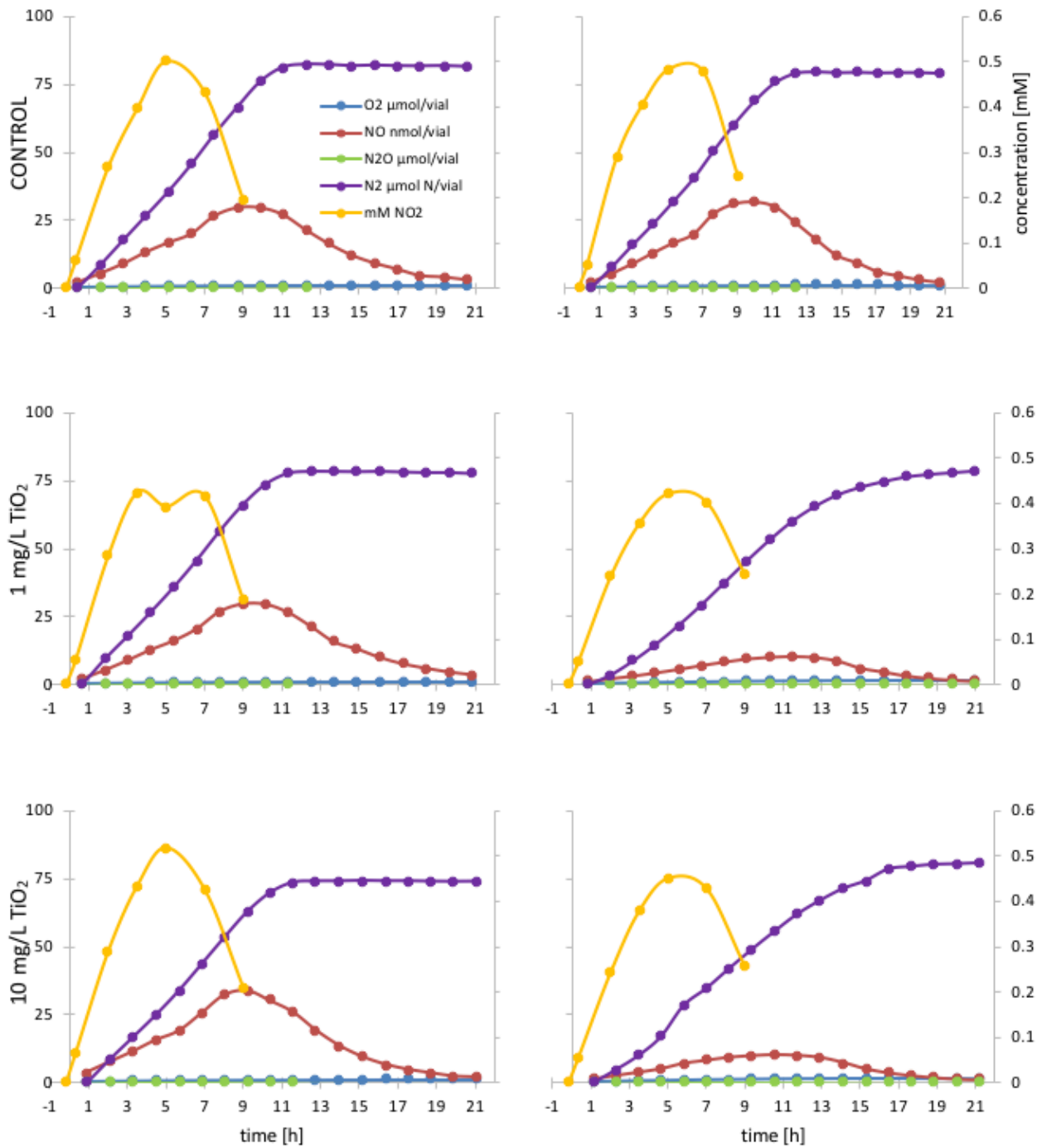


Figure C6: Kinetics of the respiration of bacterial consortium located in biofilm after exposure to TiO_2 NPs with various concentrations. Each plot represents one sample.

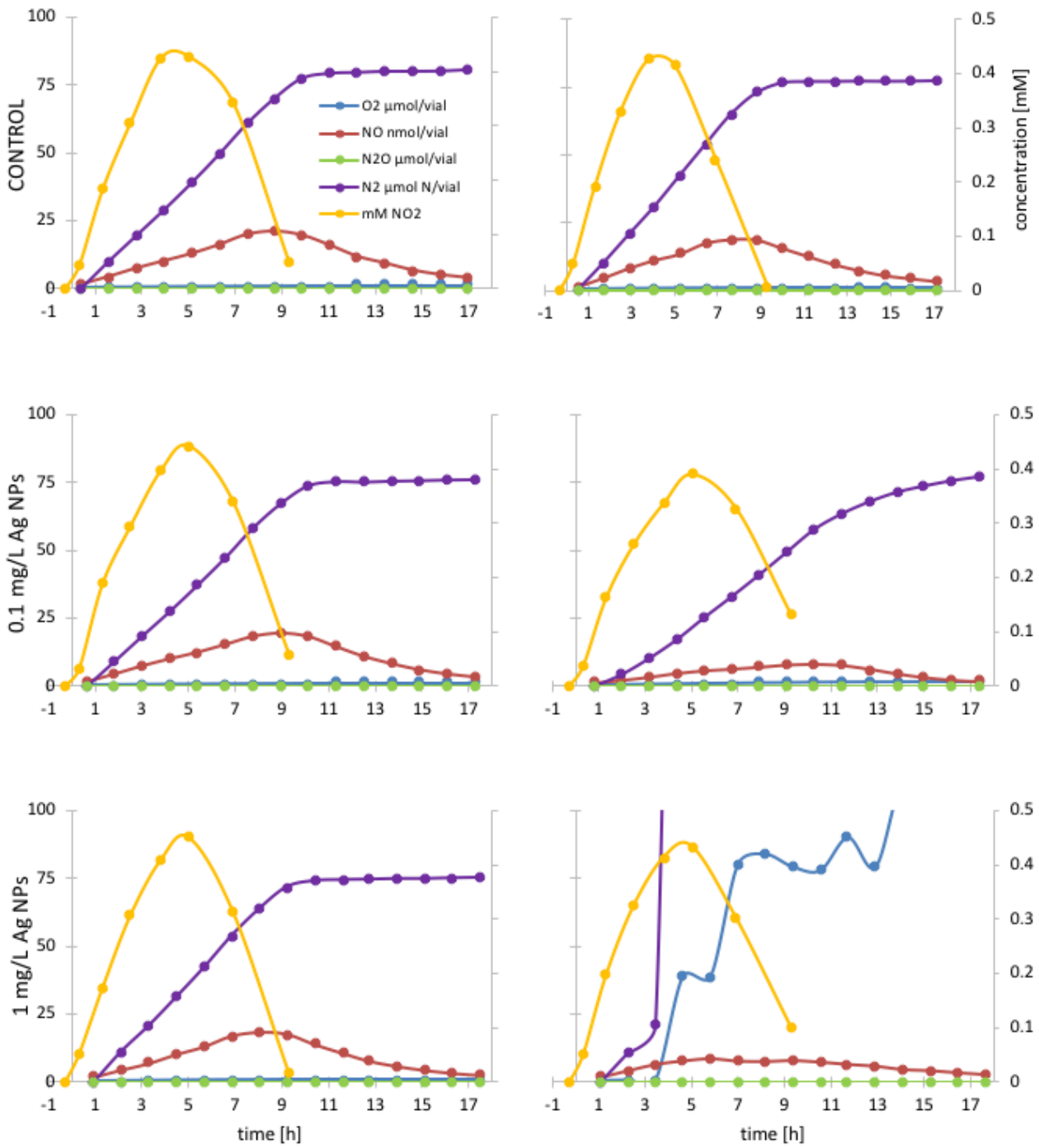


Figure C7: Kinetics of the respiration of bacterial consortium located in biofilm after exposure to Ag NPs with various concentrations. Each plot represents one sample.



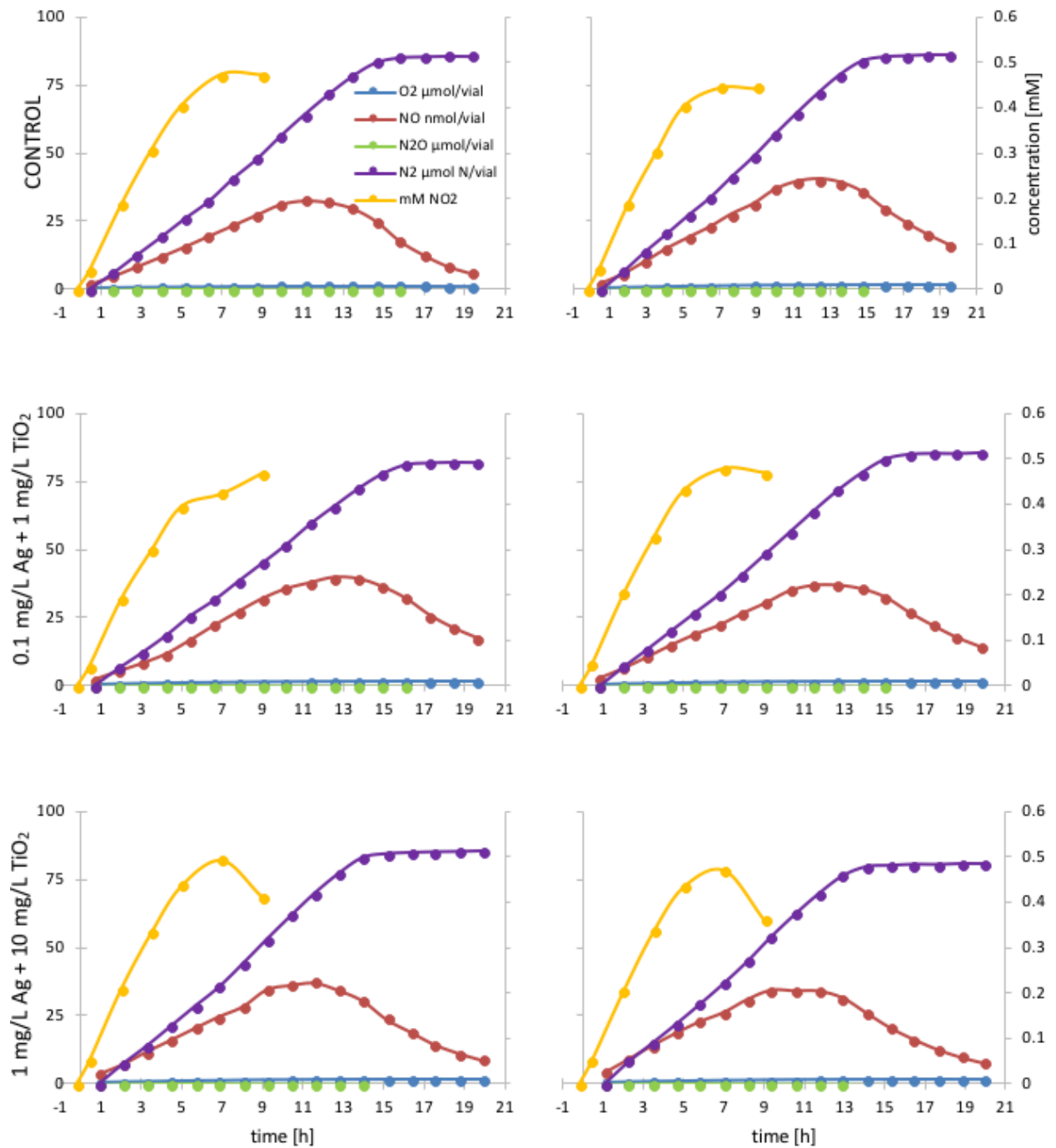


Figure C8: Kinetics of the respiration of bacterial consortium located in biofilm after exposure to combination of TiO_2 and Ag NPs with various concentrations. Each plot represents one sample.

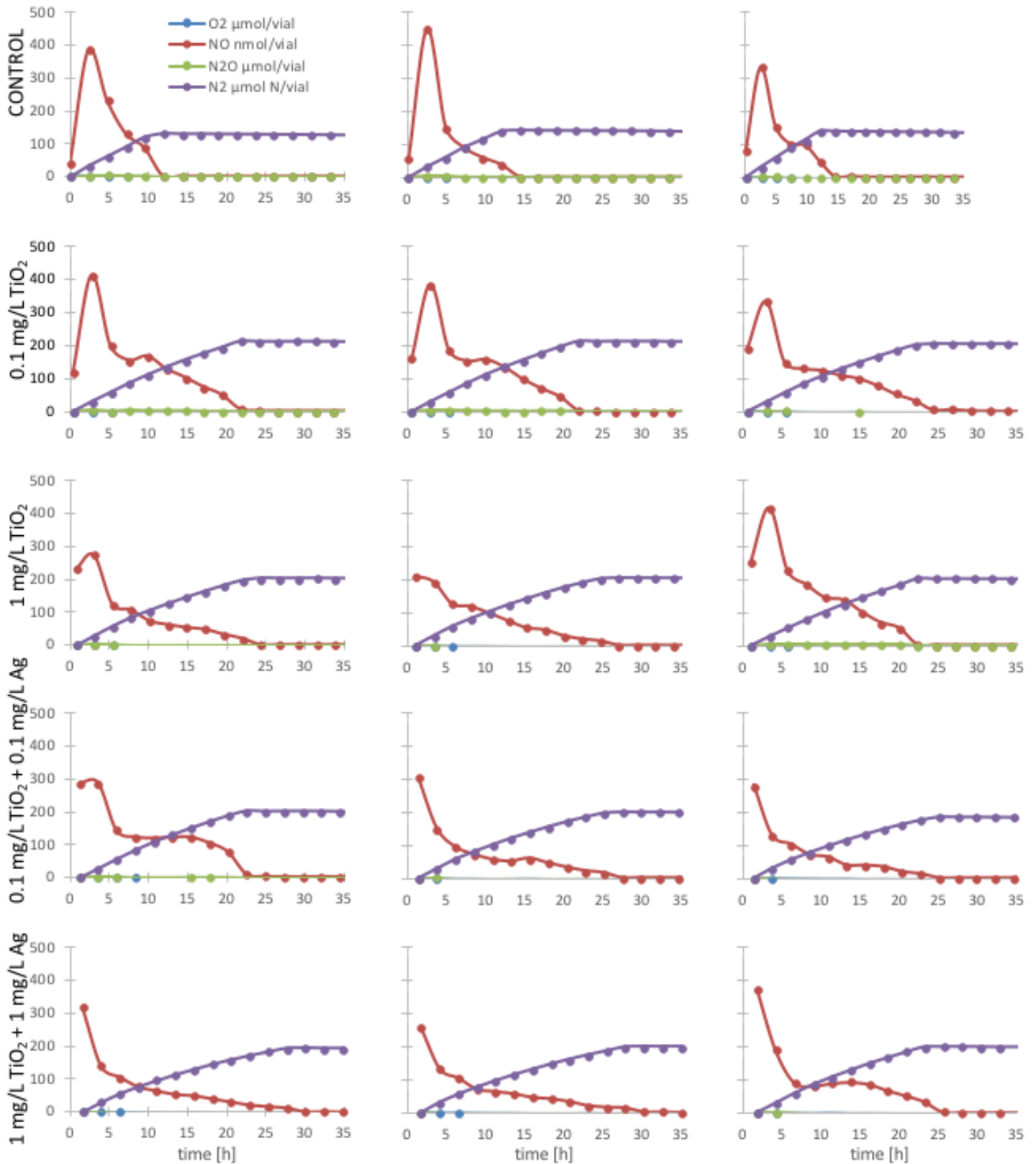


Figure C9: Kinetics of the respiration of bacterial community located in activated sludge after exposure to TiO_2 and combination of TiO_2 and Ag NPs with various concentrations. Each plot represents one sample.



Appendix D

Table D1: Analysis of 95% O_2 consumption by *P. denitrificans* after exposure to TiO_2 NPs in time. No significant variation was observed.

TiO_2 [mg/L]	control	0.1	1	10
Time when more	20	20	20	18
than 95% of O_2	18	20	20	18
was consumed [h]	20	20	20	18
mean + SD	19.3 ± 1.15	20.0 ± 0.00	20.0 ± 0.00	18.0 ± 0.00

Table D2: Analysis of 95% O_2 consumption by *T. linaloolentis* after exposure to TiO_2 NPs in time. No significant variation was detected.

TiO_2 [mg/L]	control	0.01	0.1	1	10
Time when more	16.6	16.6	16.6	16.6	16.6
than 95% of O_2	16.6	16.6	14.2	16.6	19
was depleted [h]	16.6	16.6	16.6	19	19
mean + SD	16.6 ± 0.00	16.6 ± 0.00	15.8 ± 1.39	17.4 ± 1.39	18.2 ± 1.39



Table D3: Analysis of *NO* maximal accumulation by *P. denitrificans* after exposure to *TiO₂* NPs in time. No significant variation was observed.

<i>TiO₂</i> [mg/L]	control	0.1	1	10
Time of maximum accumulation of <i>NO</i> [h]	22	24	22	22
	22	24	22	22
	24	22	24	22
mean + SD	22.7 ± 1.15	23.3 ± 1.15	22.7 ± 1.15	22.0 ± 0.00

Table D4: Analysis of *NO* maximal accumulation by *T. linaloolentis* after exposure to *TiO₂* NPs in time. No significant variation was observed.

<i>TiO₂</i> [mg/L]	control	0.01	0.1	1	10
Time of max. accumulation of <i>NO</i> [h]	26.1	23.7	26.1	26.1	23.7
	28.5	26.1	21.3	28.5	28.5
	23.7	28.5	28.5	30.5	23.7
mean + SD	26.1 ± 2.40	26.1 ± 2.40	25.3 ± 3.67	28.4 ± 2.20	25.3 ± 2.77

Table D5: Analysis of 90% *O₂* consumption by *N. europaea* after exposure to *Ag* NPs in time. No significant variation was detected between 0.1 - 10 $\mu\text{g/L}$ concentrations. NC = no consumption.

<i>Ag</i> [$\mu\text{g/L}$]	control	0.1	1	10	100	1000
Time of maximum accumulation of <i>NO</i> [h]	199.5	205.6	211.6	241.9	NC	
	217.17	211.6	205.6	211.6		
mean + SD	208.6 ± 12.87	208.6 ± 4.24	208.6 ± 4.24	226.8 ± 21.43		

Table D6: Analysis of *NO₂⁻* maximal accumulation by *N. europaea* after exposure to *Ag* NPs in time. No significant variation was observed between 0.1 - 10 $\mu\text{g/L}$. LV = significantly low values.

<i>Ag</i> [$\mu\text{g/L}$]	control	0.1	1	10	100	1000
Time of maximum accumulation of <i>NO₂⁻</i> [h]	264	264	264	264	LV	
	240	240	264	264		
mean + SD	252.0 ± 16.97	252.0 ± 16.97	264.0 ± 0.00	264.0 ± 0.00		



Table D7: Analysis of times when more than 95% of N_2 was accumulated by bacterial consortium from biofilm after exposure to TiO_2 NPs. No significant variation was detected.

TiO_2 [mg/L]	control	1	10
Time when more than 95% of	11.1	11.1	11.1
N_2 was accumulated [h]	11.1	15.8	15.8
mean + SD	11.1 ± 0.00	13.45 ± 3.32	13.45 ± 3.32

Table D8: Analysis of NO maximal accumulation by bacterial consortium from biofilm after exposure to TiO_2 NPs in time. No significant variation was observed.

TiO_2 [mg/L]	control	1	10
Time of maximum	9.9	8.7	8.7
accumulation of NO [h]	9.9	11.1	9.9
mean + SD	9.9 ± 0.00	9.9 ± 1.70	9.3 ± 0.85

Table D9: Analysis of NO_2^- maximal accumulation by bacterial consortium from biofilm after exposure to TiO_2 NPs in time. No significant variation was observed.

TiO_2 [mg/L]	control	1	10
Time of maximum	5	3.5	5
accumulation of NO_2^- [h]	5	5	5
mean + SD	5.0 ± 0.00	4.3 ± 1.06	5.0 ± 0.00

Table D10: Analysis of times when more than 95% of N_2 was accumulated by bacterial consortium from biofilm after exposure to Ag NPs. No significant variation was detected.

Ag [mg/L]	control	0.1	1
Time when more than 95% of	9.9	9.9	8.7
N_2 was accumulated [h]	9.9	14.6	X
mean + SD	9.9 ± 0.00	12.25 ± 3.32	8.7



Table D11: Analysis of NO maximal accumulation by bacterial consortium from biofilm after exposure to Ag NPs in time. No significant variation was observed. X = sample problem.

Ag [mg/L]	control	0.1	1
Time of maximum accumulation of NO [h]	8.7	8.7	7.5
mean + SD	8.1 ± 0.85	9.3 ± 0.85	7.5

Table D12: Analysis of NO_2^- maximal accumulation by bacterial consortium from biofilm after exposure to Ag NPs in time. No significant variation was noticed.

Ag [mg/L]	control	0.1	1
Time of maximum accumulation of NO_2^- [h]	5	5	5
mean + SD	4.4 ± 0.85	5.0 ± 0.00	5.0 ± 0.00

Table D13: Analysis of times when more than 95% of N_2 was accumulated by bacterial consortium from biofilm after exposure to combination of TiO_2 and Ag NPs. No significant variation was detected.

$TiO_2 + Ag$ [mg/L]	control	1 + 0.1	10 + 1
Time when more than 95% of N_2 was accumulated [h]	14.6	15.8	13.4
mean + SD	14.6 ± 0.00	15.2 ± 0.85	13.4 ± 0.00



Table D14: Analysis of NO maximal accumulation by bacterial consortium from biofilm after exposure to combination of TiO_2 and Ag NPs in time. No significant variation was observed.

$TiO_2 + Ag$ [mg/L]	control	1 + 0.1	10 + 1
Time of maximum accumulation of NO [h]	11.1	12.3	11.1
mean + SD	11.7 ± 0.85	12.3 ± 0.00	9.9 ± 1.70

Table D15: Analysis of NO_2^- maximal accumulation by bacterial consortium from biofilm after exposure to combination of TiO_2 and Ag NPs in time. No significant variation was noticed.

$TiO_2 + Ag$ [mg/L]	control	1 + 0.1	10 + 1
Time of maximum accumulation of NO [h]	7	9	7
mean + SD	7.0 ± 0.00	8.0 ± 1.41	7.0 ± 0.00

Table D16: Analysis of times when more than 95% of N_2 was accumulated by bacteria community located in activated sludge after exposure to TiO_2 and combination of TiO_2 and Ag NPs without control sample. Weird control not included in the statistical analysis (red).

[mg/L]	control	0.1 TiO_2	1 TiO_2	0.1 $TiO_2 + Ag$	1 $TiO_2 + Ag$
Time when more than 95% of N_2 was accumulated [h]	11.9	21.3	21.3	21.3	26.1
mean + SD	11.9 ± 0.00	21.3 ± 0.00	22.1 ± 1.39	22.1 ± 1.39	24.5 ± 2.77



Appendix E

Attached CD contents:

- Master thesis text:
master_thesis_2018_Filip_Hrncirik.pdf
- Data sheets:
nitrite_analysis.xlsx
GC_results_analysis.xlsx
statistical_analysis.pzfx
FISH_analysis.xlsx

